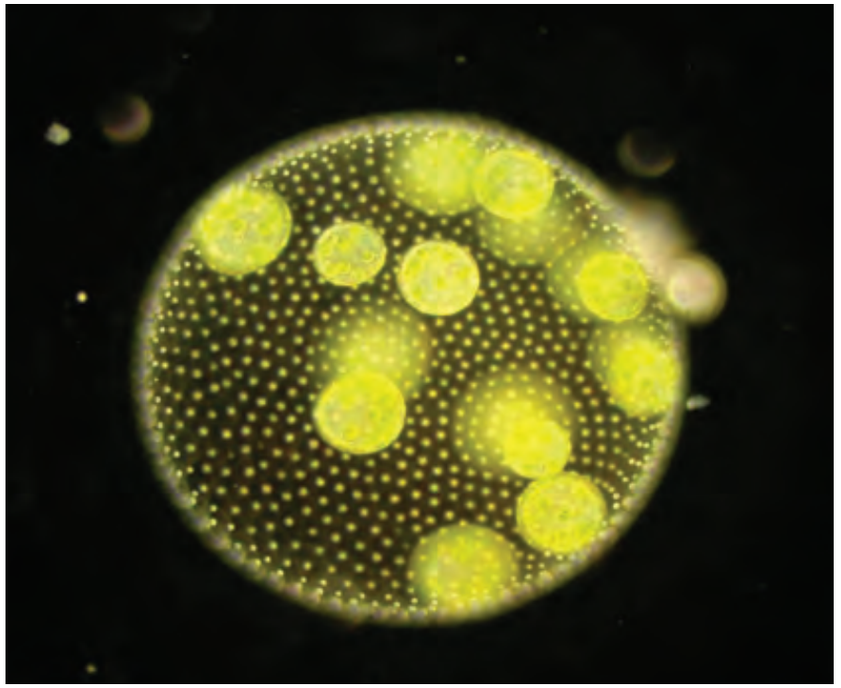
Phototaxis in Volvox

7.74/8.590/20.416



dunkel@mit.edu

Fidelity of adaptive phototaxis

Knut Drescher, Raymond E. Goldstein[1], and Idan Tuval

Department of Applied Mathematics and Theoretical Physics, University of Cambridge, Wilberforce Road, Cambridge CB3 0WA, United Kingdom

Edited by Harry L. Swinney, University of Texas, Austin, TX, and approved May 6, 2010 (received for review January 28, 2010)

www.pnas.org/cgi/doi/10.1073/pnas.1000901107

PNAS | **June 22, 2010** | vol. 107 | no. 25 | **11171–11176**

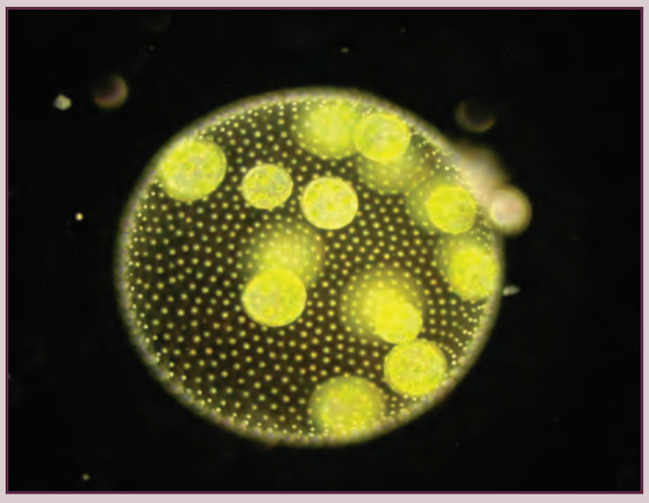
June 22, 2010 | vol. 107 | no. 25 | 11147–11650

PNAS

Proceedings of the National Academy of Sciences of the United States of America www.pnas.org

In This Issue

Moving to the light



Multicellular colony *Volvox carteri*.

To optimize photosynthesis, algae such as *Volvox carteri* swim toward or away from sunlight. To execute this motion, known as phototaxis, these microorganism colonies must coordinate the beating of thousands of flagellated cells despite the organism's lack of a central nervous system. Using analytical and empirical methods, Knut Drescher et al. (pp. 11171–11176) demonstrate that *V. carteri* spins about its swimming direction at a frequency that likely coevolved with the organism's flagellar kinetics to maximize photoreactivity. To characterize the flagellar beating of the organisms, the authors measured the fluid velocities produced by the flagella and modeled the motion with hydrodynamic equations. Using the model, the authors identified a theoretical optimal spinning frequency and tested the finding experimentally by observing how well the algae swam in media with increased viscosities that inhibited the organism's ability to spin. According to the authors, the experiments demonstrated that with a decreased rotation rate the algae were unable to execute phototaxis as accurately as before, suggesting that in *V. carteri*, flagellar beating and spinning are linked adaptations. By better understanding how simple organisms coordinate multicellular processes, the findings may provide insight into key evolutionary steps that eventually led to higher organisms with central nervous systems. — T.J.

dunkel@math.mit.edu



Knut Drescher

MPI Marburg



Idan Tuval

Mediterranean
Institute for
Advanced Studies



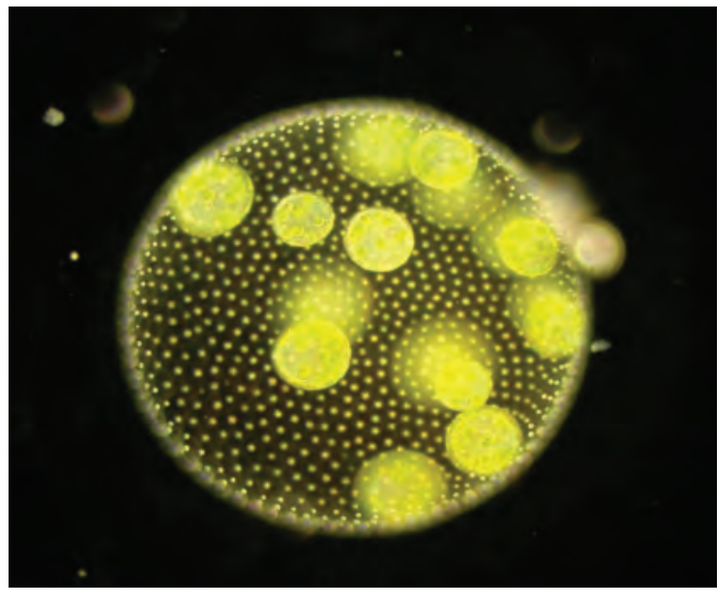
Ray Goldstein

Cambridge

dunkel@math.mit.edu

Why is Volvox interesting ?

- germ-soma differentiation
- interesting asexual reproduction ‘technique’
- metachronal waves
- locomotion
- phototaxis



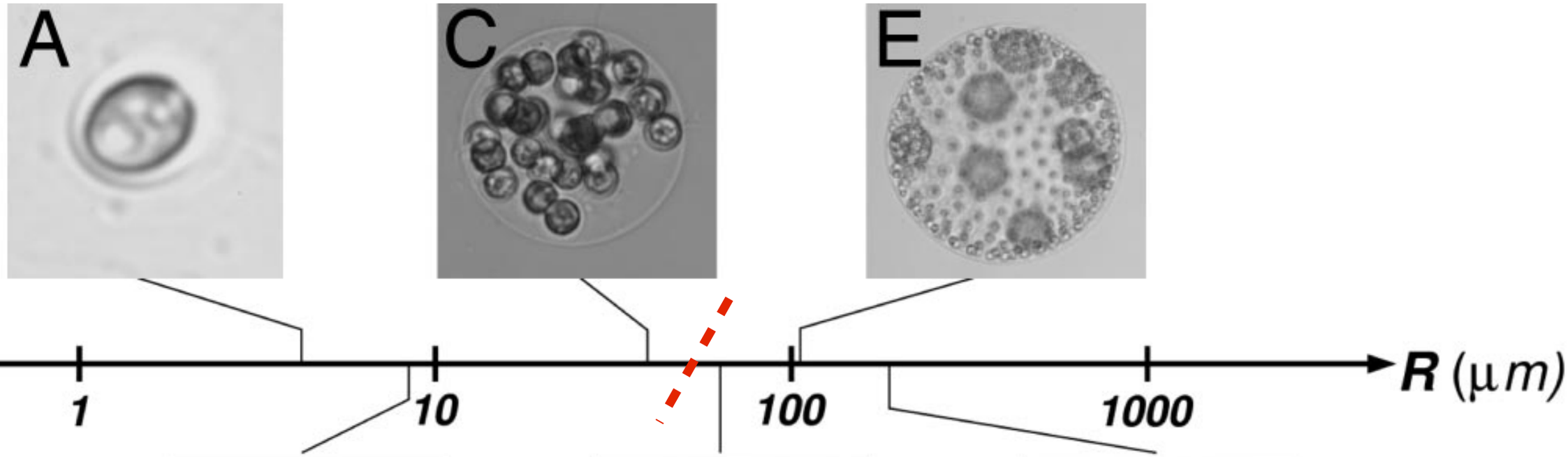
dunkel@math.mit.edu

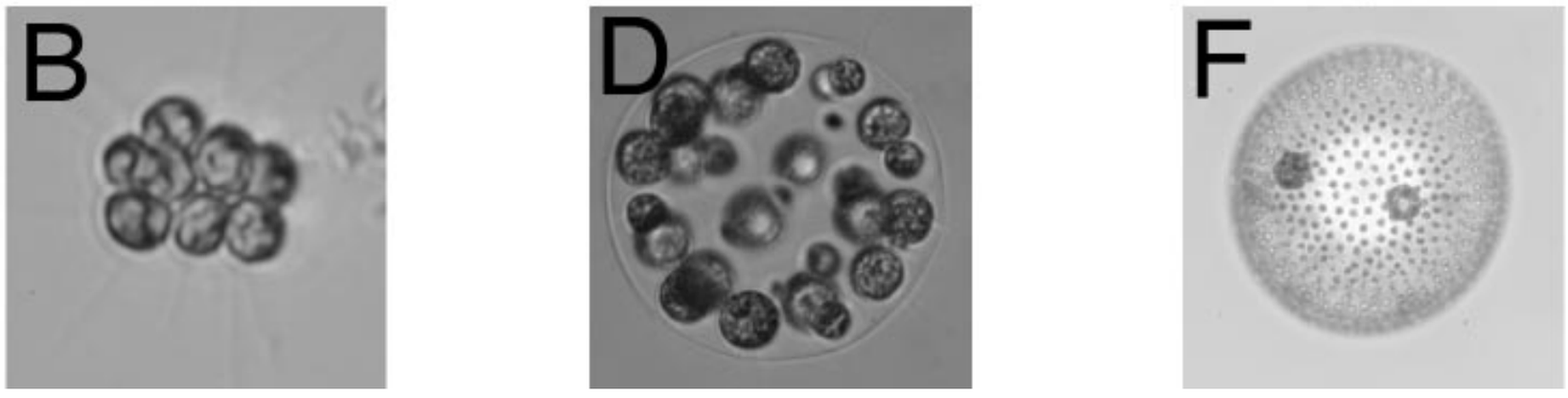
Evolution of multicellularity

Chlamydomonas reinhardtii

Eudorina elegans

Volvox carteri





Gonum pectorale

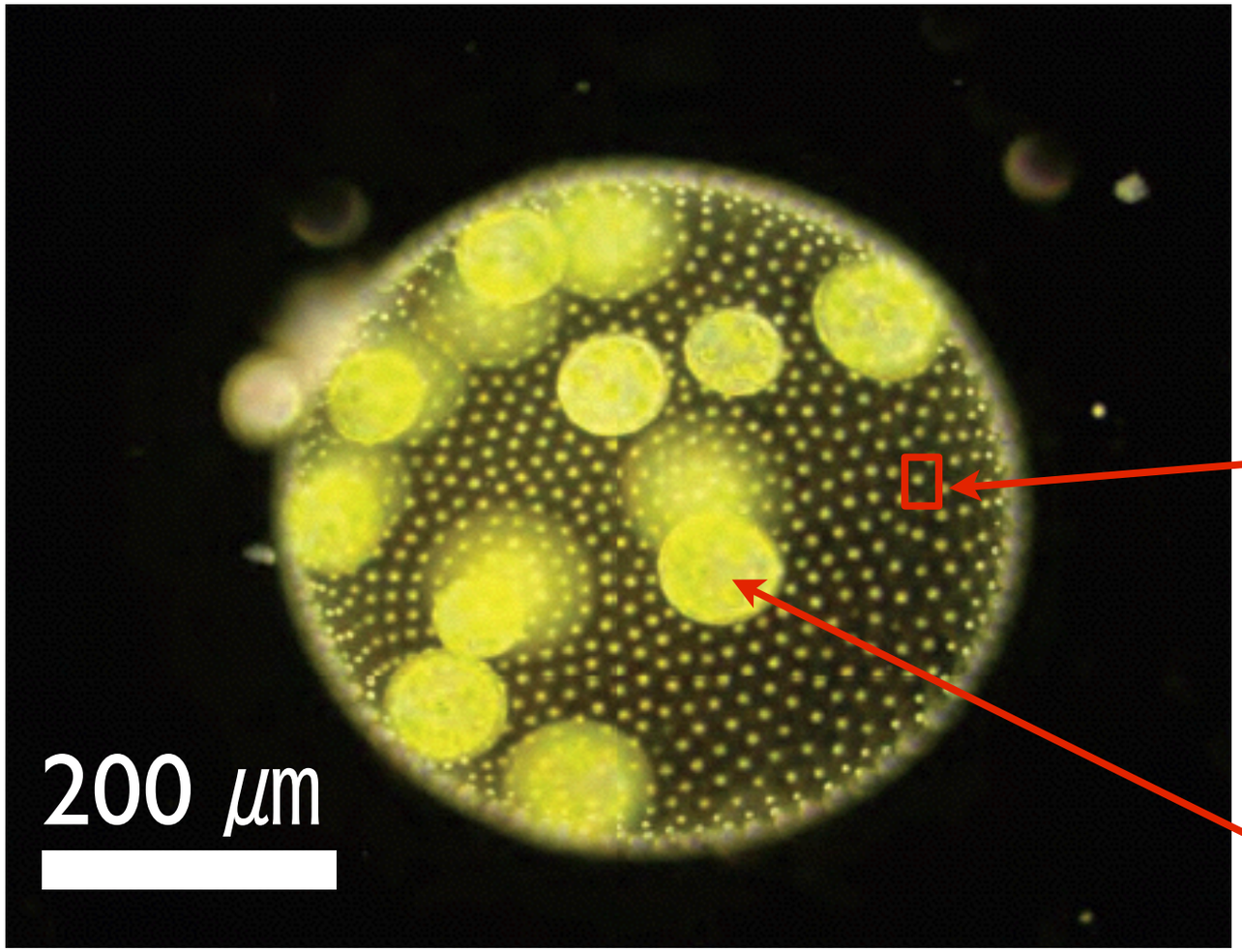
Pleodorina californica

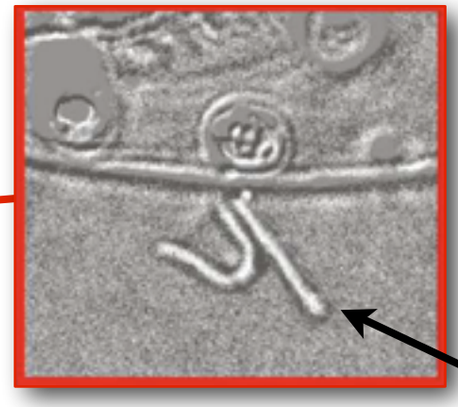
Volvox aureus

Short et al, PNAS 2013

dunkel@math.mit.edu

Volvox carteri





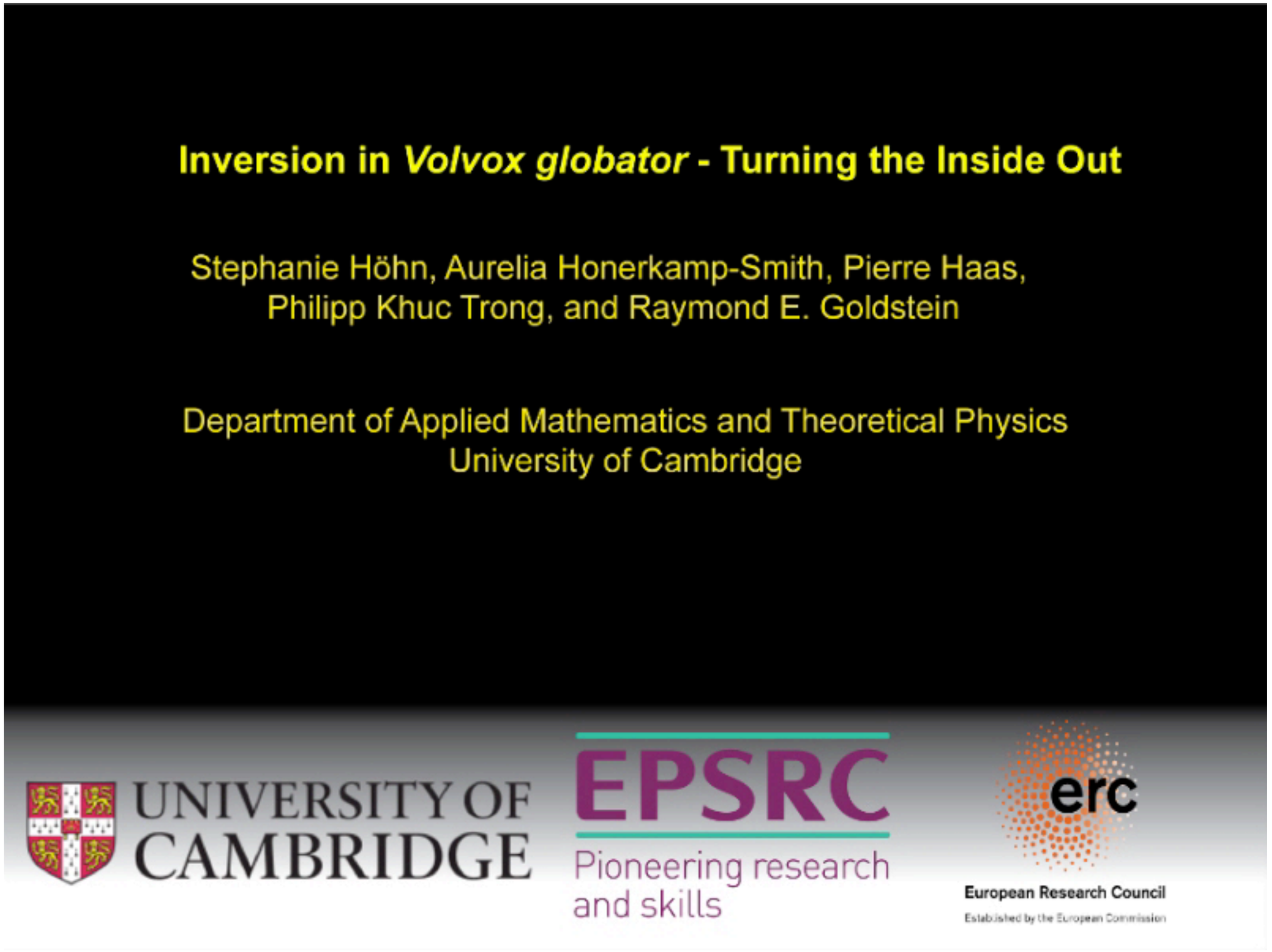
somatic cell

cilia

daughter colony from germ cell

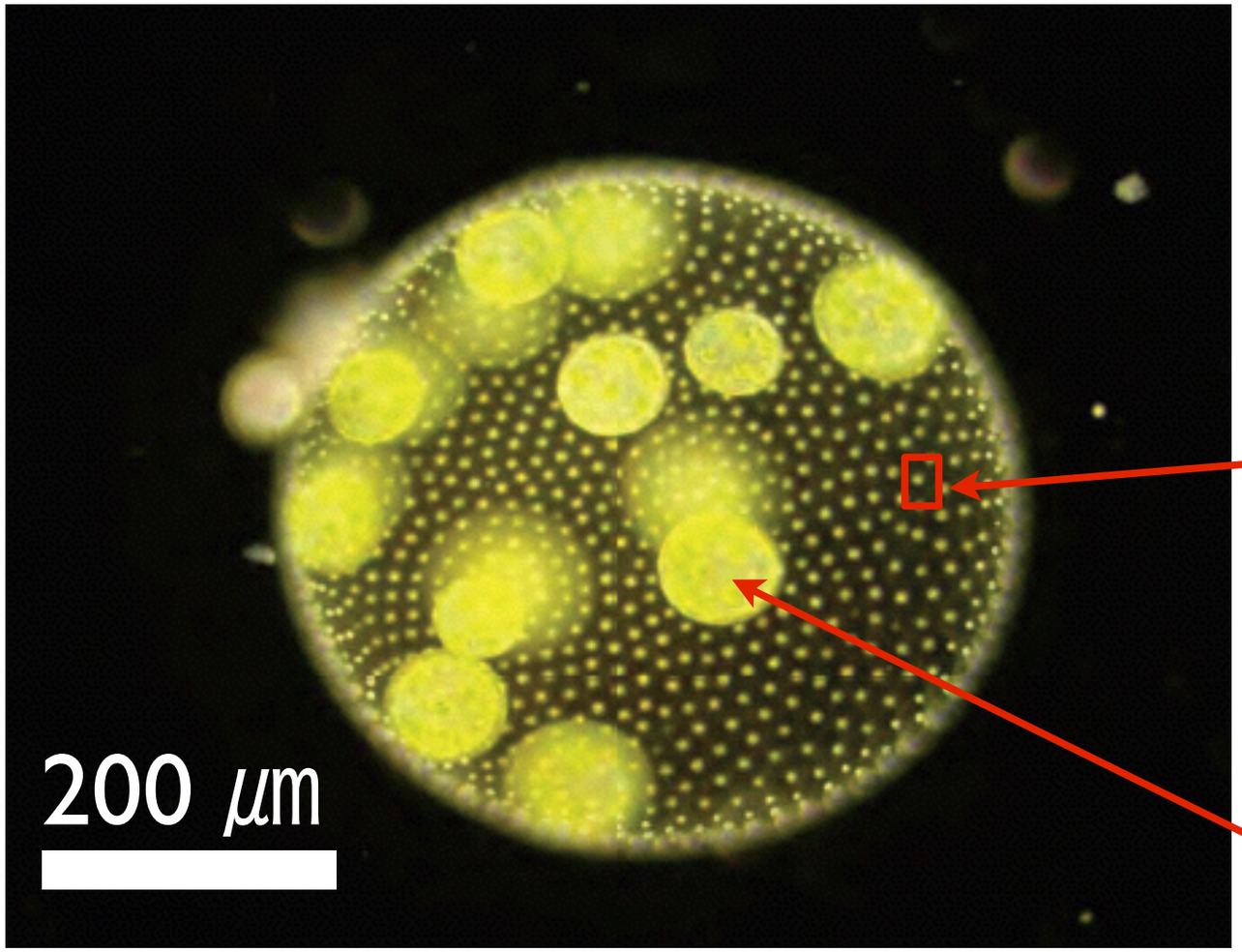
dunkel@math.mit.edu

Asexual reproduction & inversion

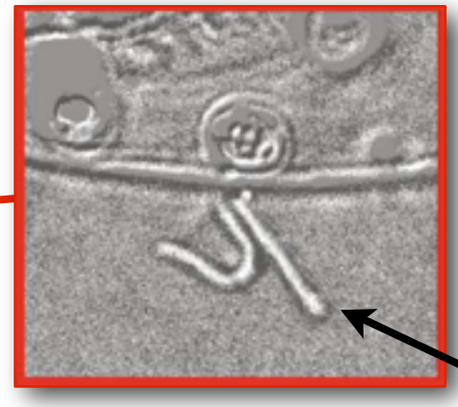


2014 Goldstein lab

dunkel@math.mit.edu



Volvox carteri



somatic cell

cilia

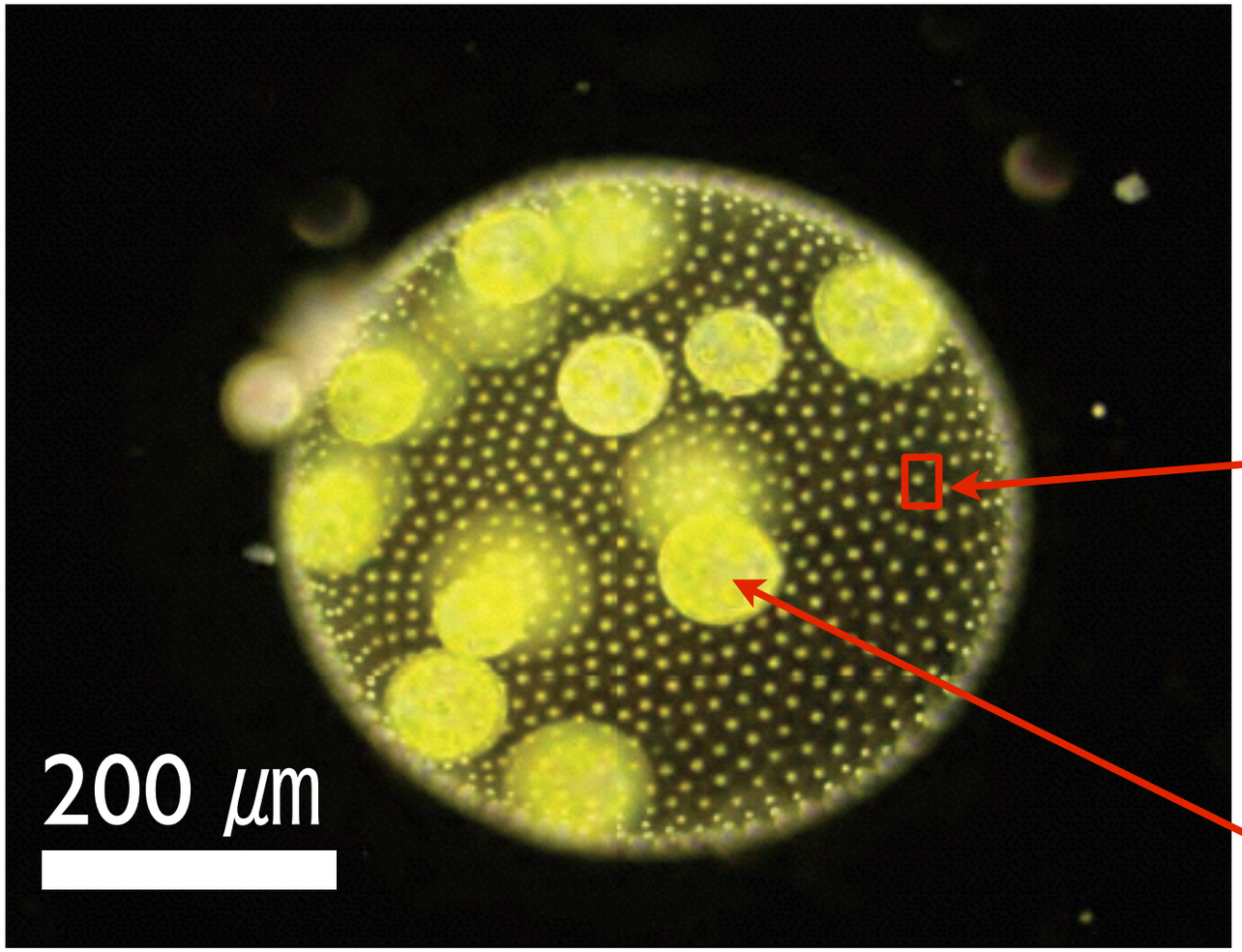
daughter colony from germ cell

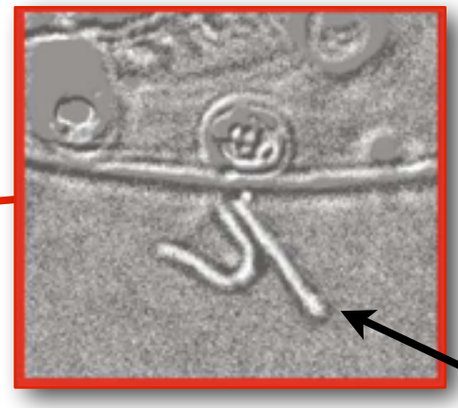
... and can dance

Drescher et al (2010) PRL

dunkel@math.mit.edu

Volvox carteri

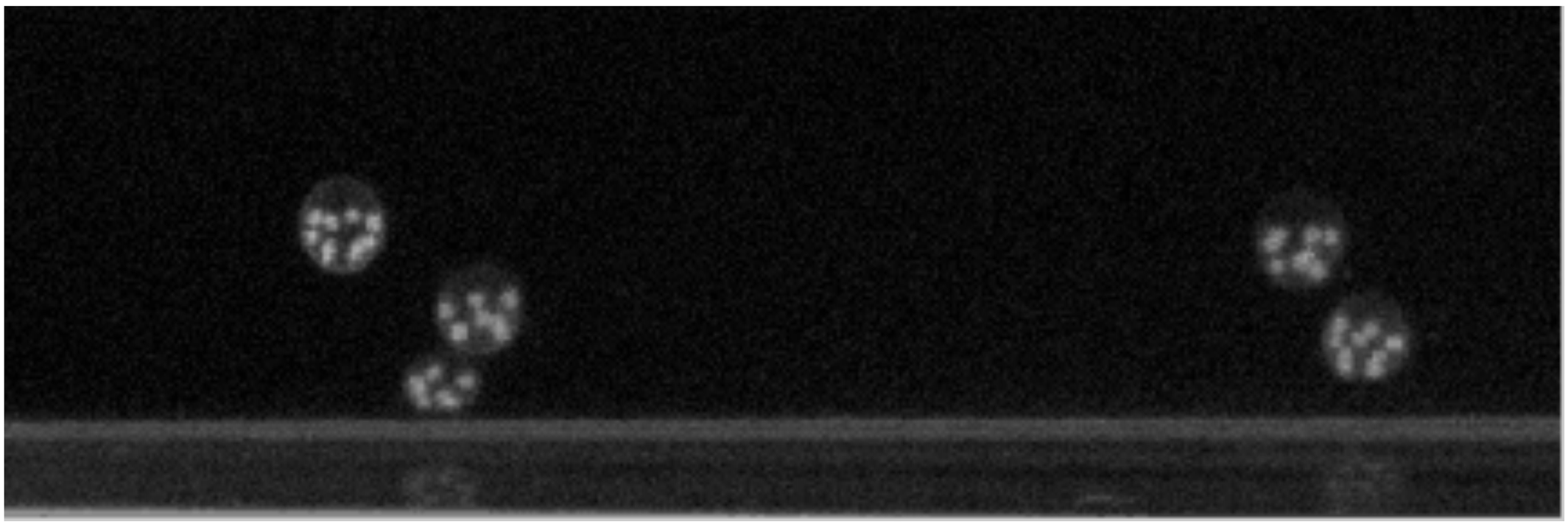




somatic cell

cilia

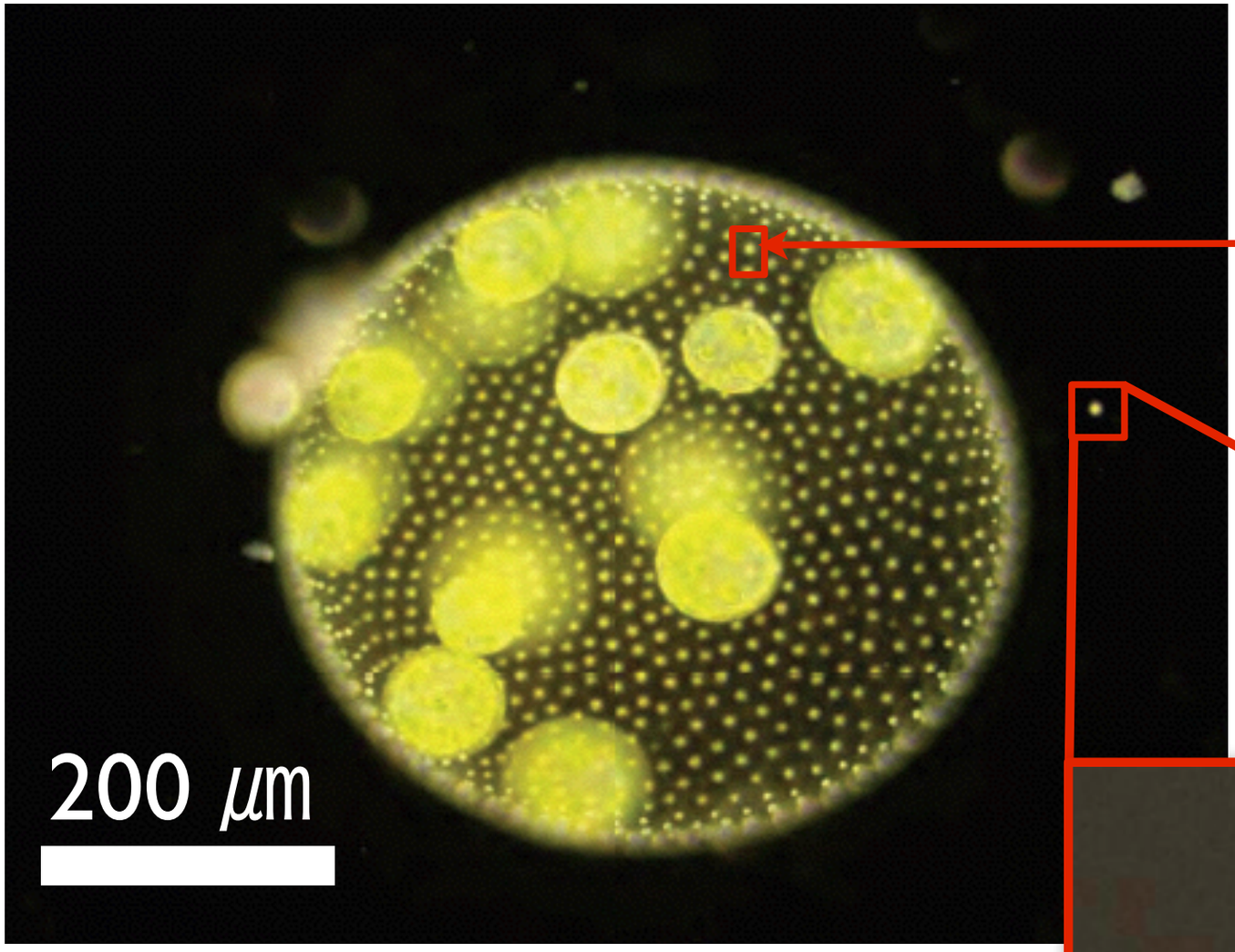
daughter colony



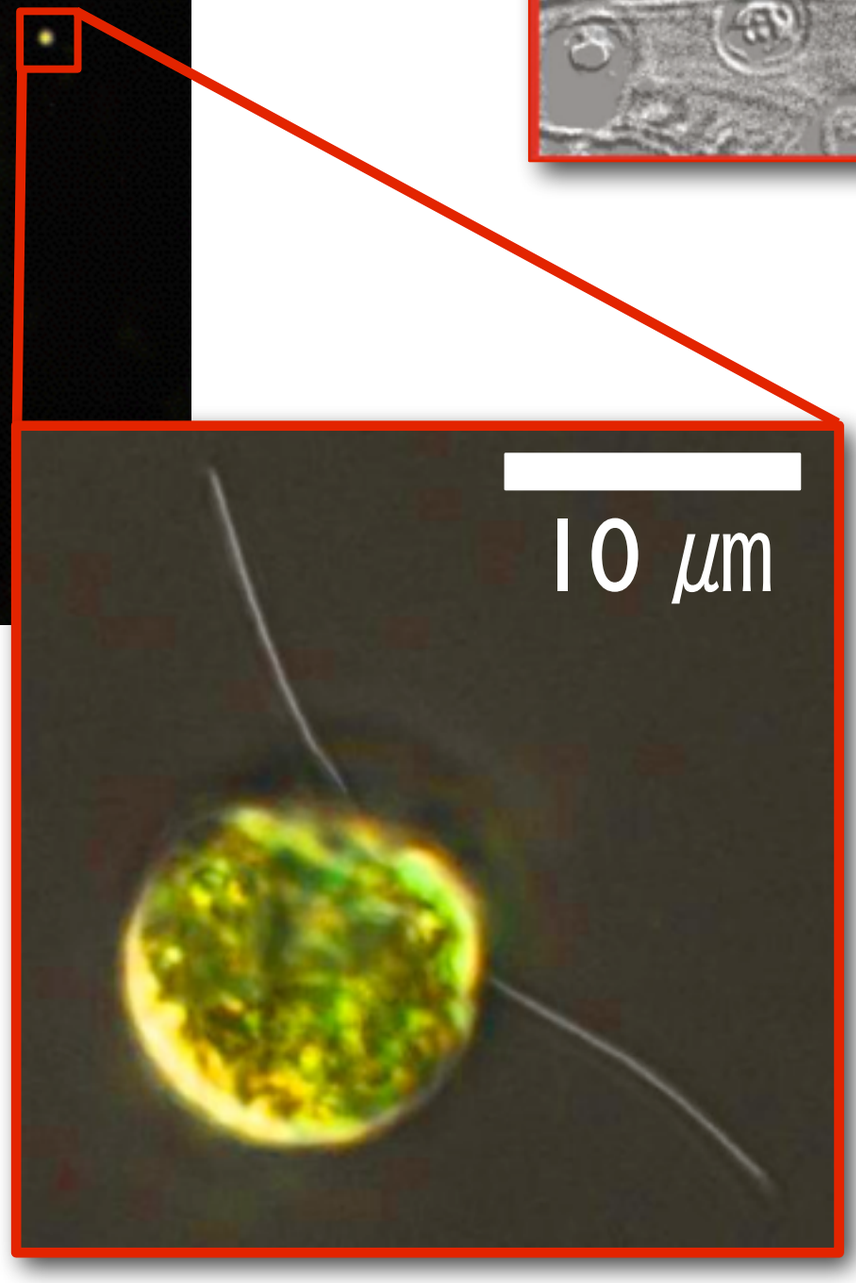
Drescher et al (2010) PRL

dunkel@math.mit.edu

Volvox carteri



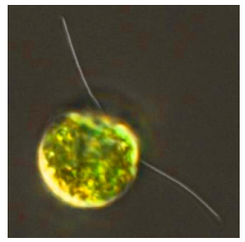


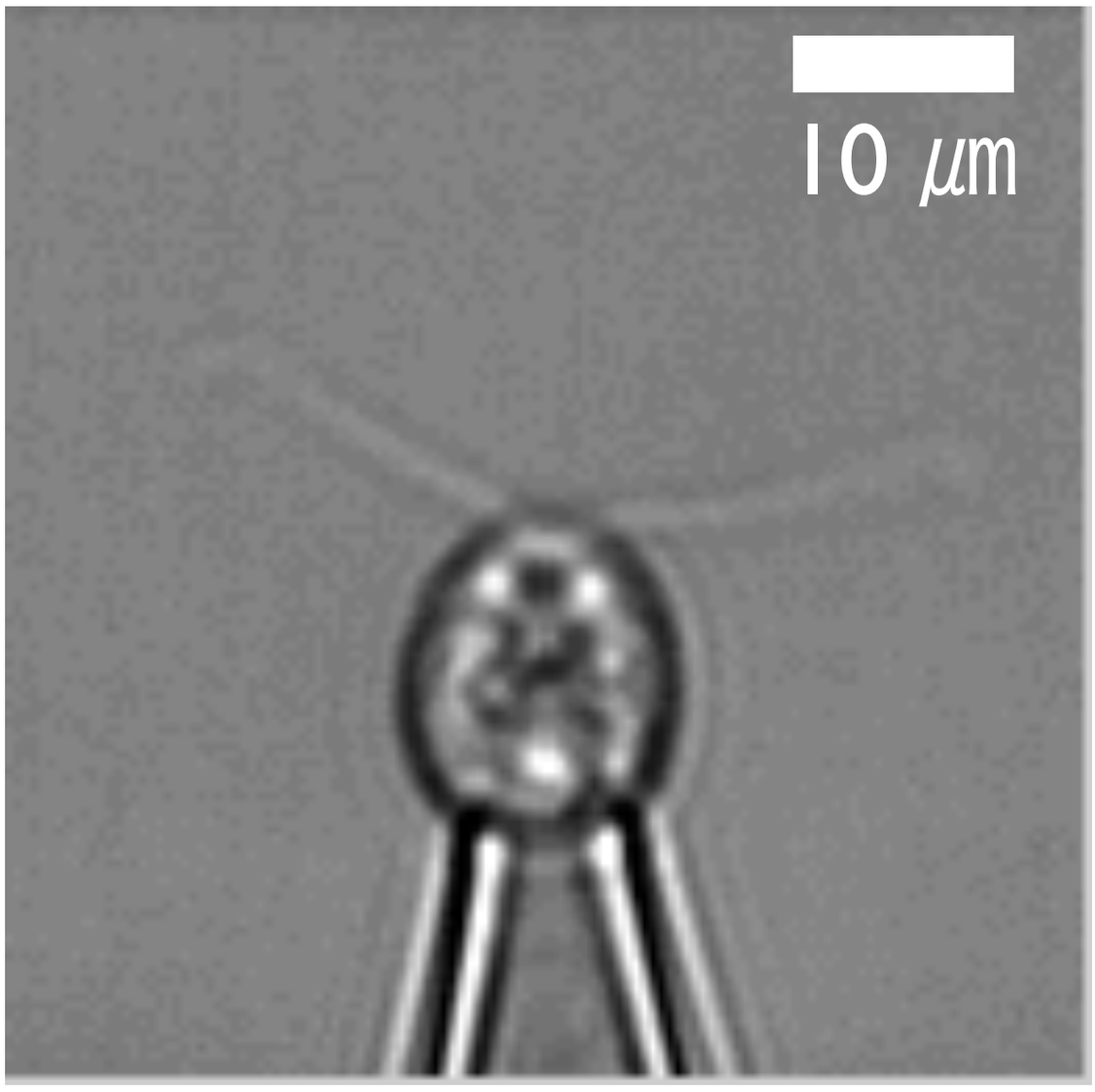


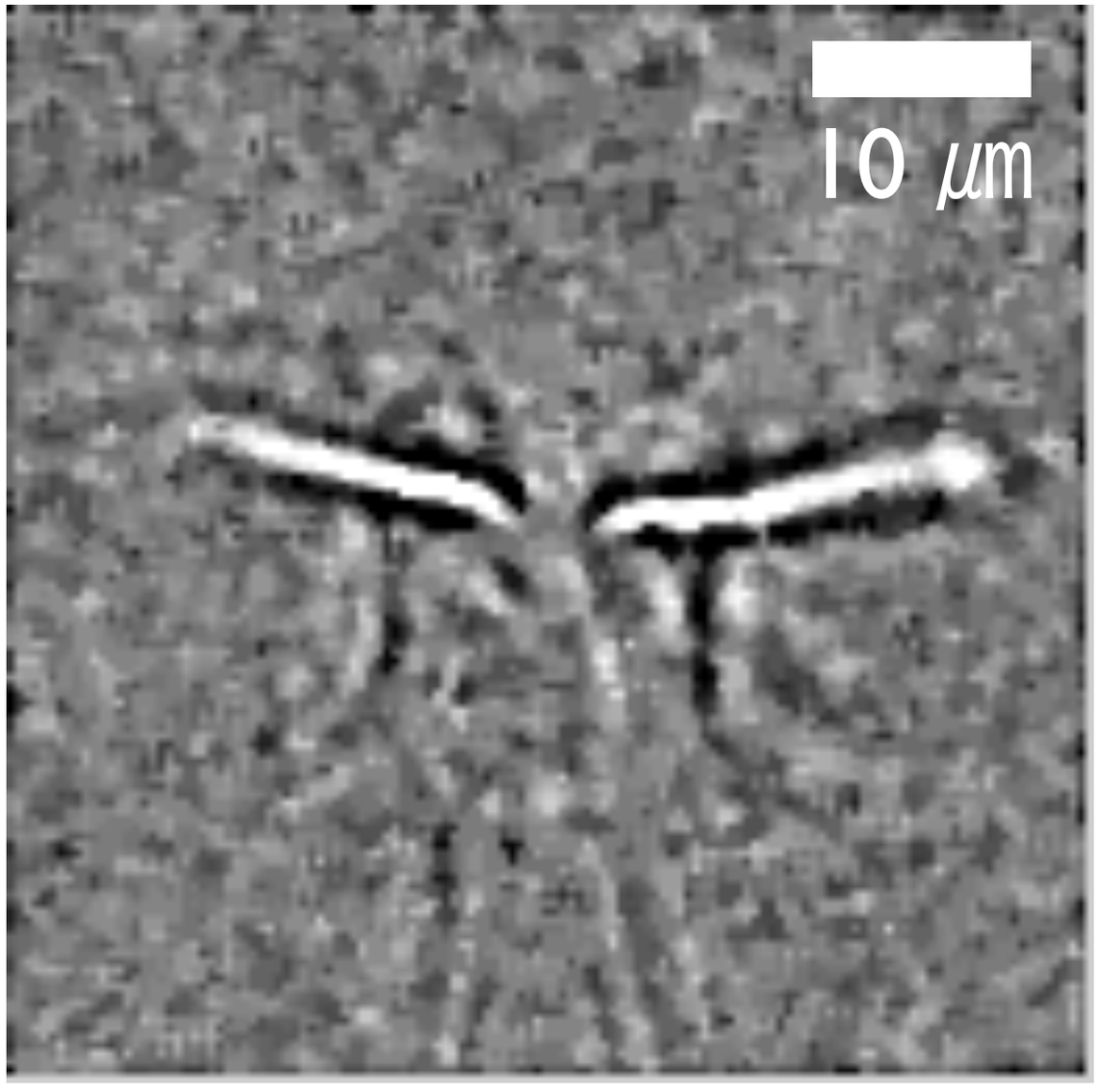
Chlamydomonas reinhardtii

dunkel@math.mit.edu

Chlamydomonas alga







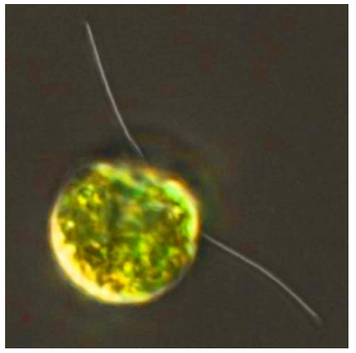
~ 50 beats / sec

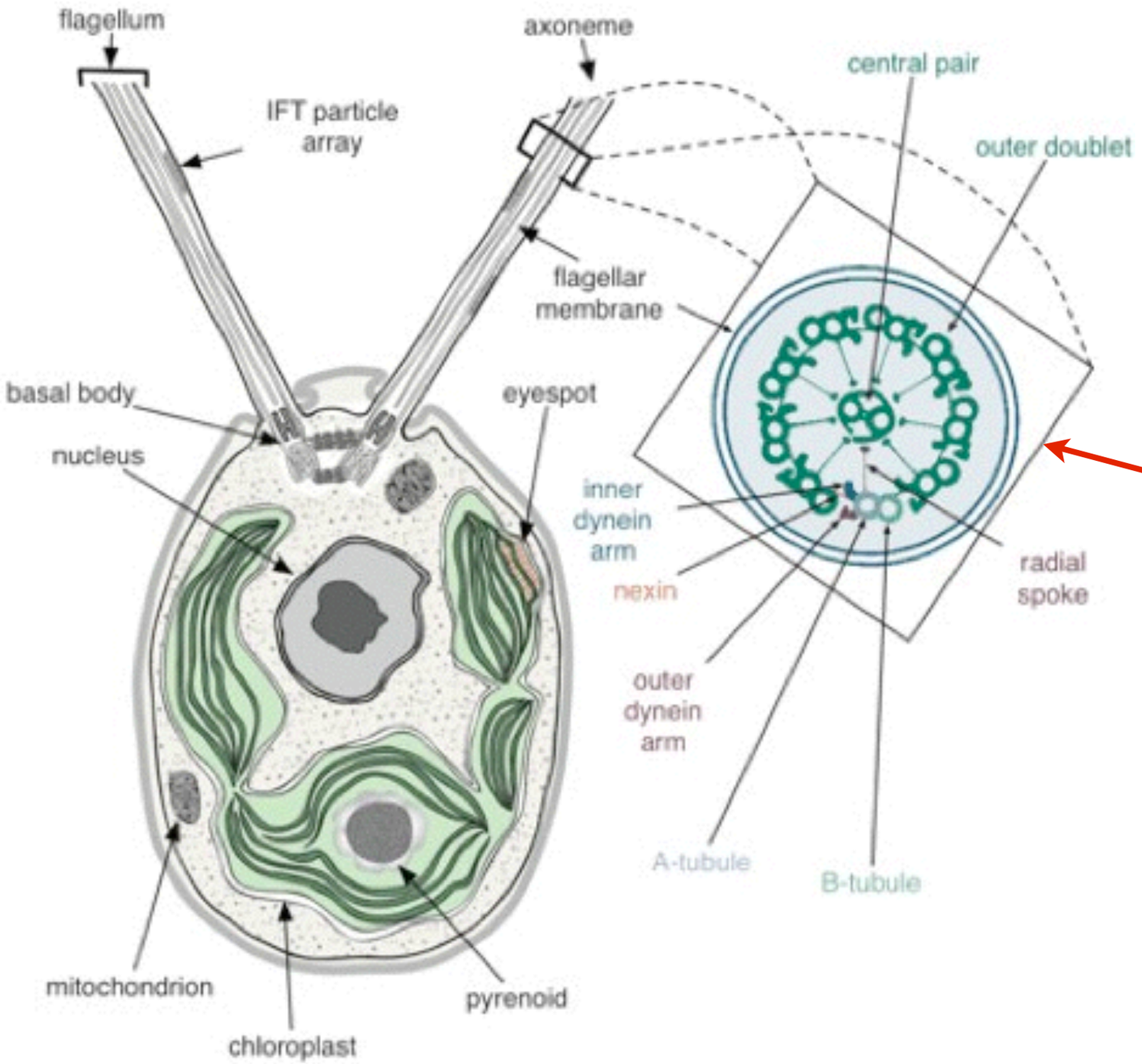
speed ~100 μm/s

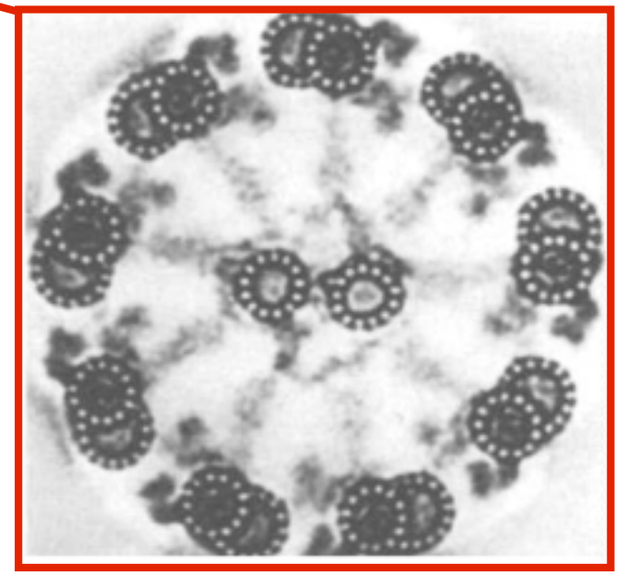
Goldstein et al (2011) PRL

dunkel@math.mit.edu

Chlamydomonas

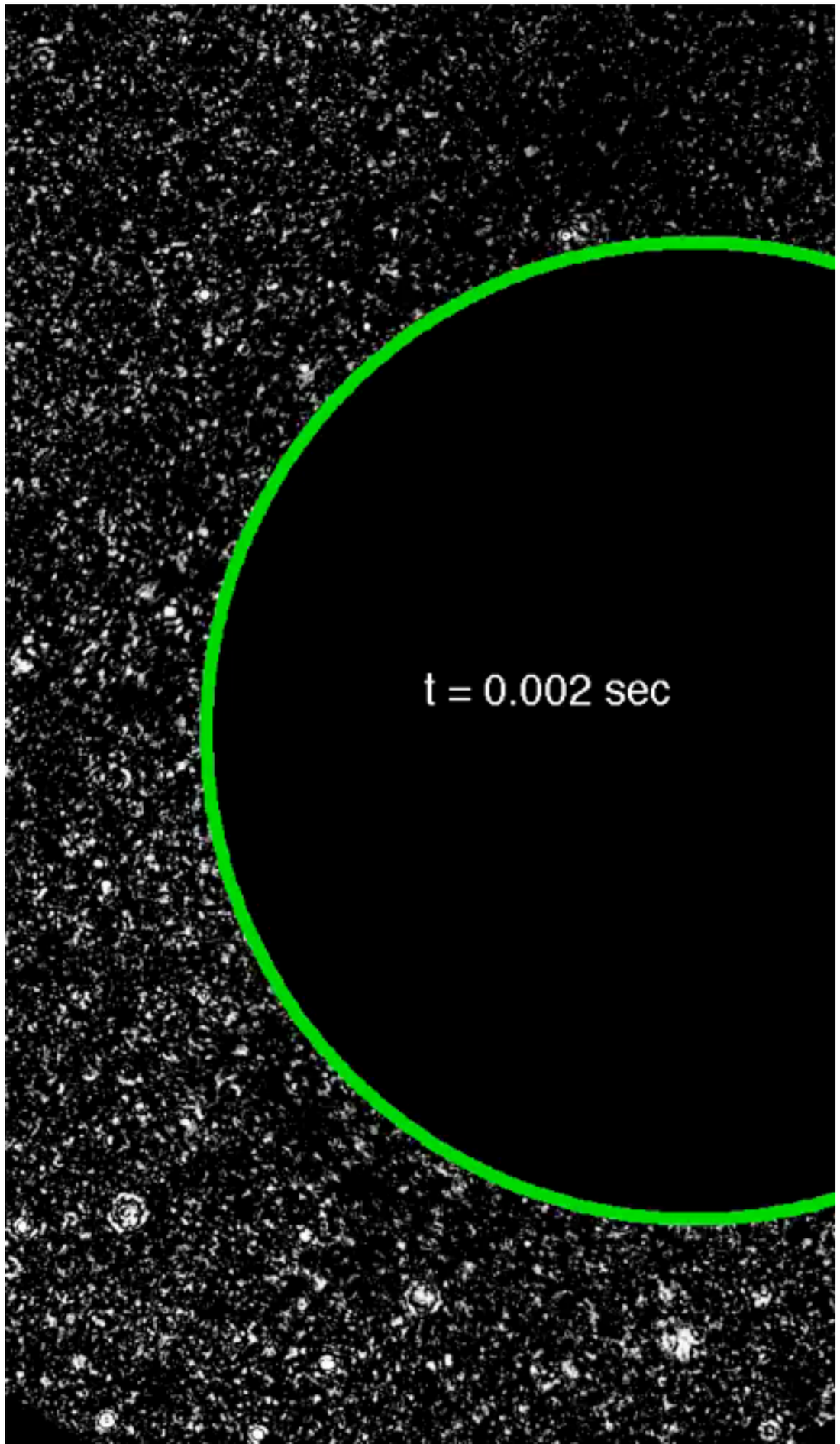






Merchant et al (2007) Science

dunkel@math.mit.edu



Model organism for studying meta-chronal waves

Brumley et al (2012) PRL

dunkel@math.mit.edu

Swimming at low Reynolds number

Navier - Stokes:

$$-\nabla p + \eta \nabla^2 \vec{v} = \rho \frac{\partial \vec{v}}{\partial t} + \rho (\vec{v} \cdot \nabla) \vec{v}$$

If $\mathcal{R} \sim UL\rho/\eta \ll 1$

Time doesn't matter. The pattern of motion is the same, whether slow or fast, whether forward or backward in time.

The Scallop Theorem



American Journal of Physics, Vol. 45, No. 1, January 1977



Geoffrey Ingram Taylor



James Lighthill

$$0 = \mu \nabla^2 \boldsymbol{u} - \nabla p + \boldsymbol{f},$$
$$0 = \nabla \cdot \boldsymbol{u}.$$

\+ time-dependent BCs

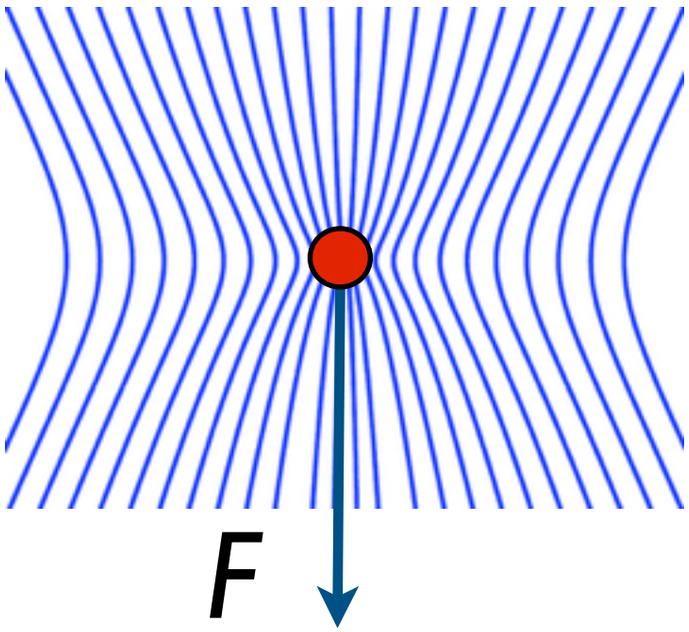


Edward Purcell

Shapere & Wilczek (1987) PRL

Superposition of singularities

stokeslet

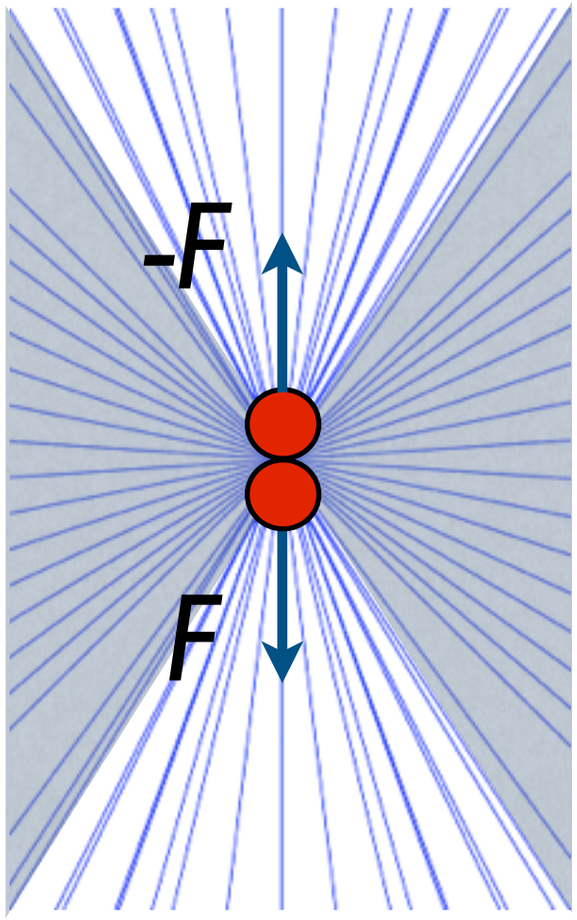


$$p(\boldsymbol{r}) = \frac{\hat{\boldsymbol{r}} \cdot \boldsymbol{F}}{4\pi r^2} + p_0$$

$$v_i(\boldsymbol{r}) = \frac{(8\pi\mu)^{-1}}{r}[\delta_{ij} + \hat{r}_i\hat{r}_j]F_j$$

flow ~ r^{-1}

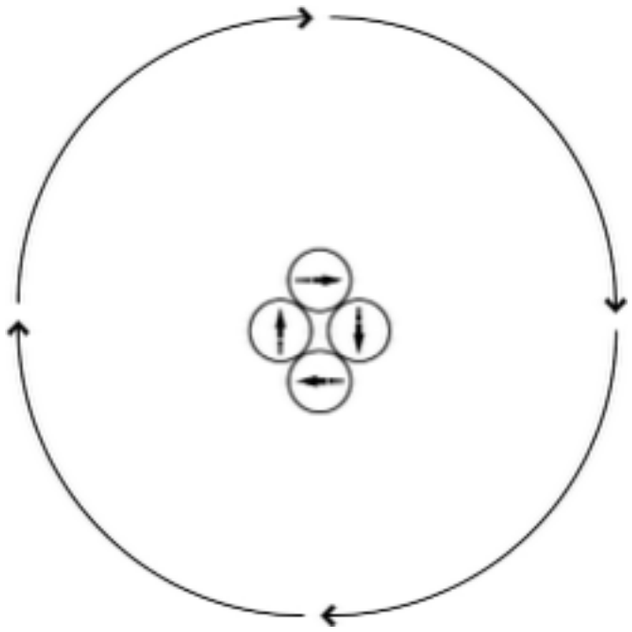
2x stokeslet =
symmetric dipole



r^{-2}

‘pusher’

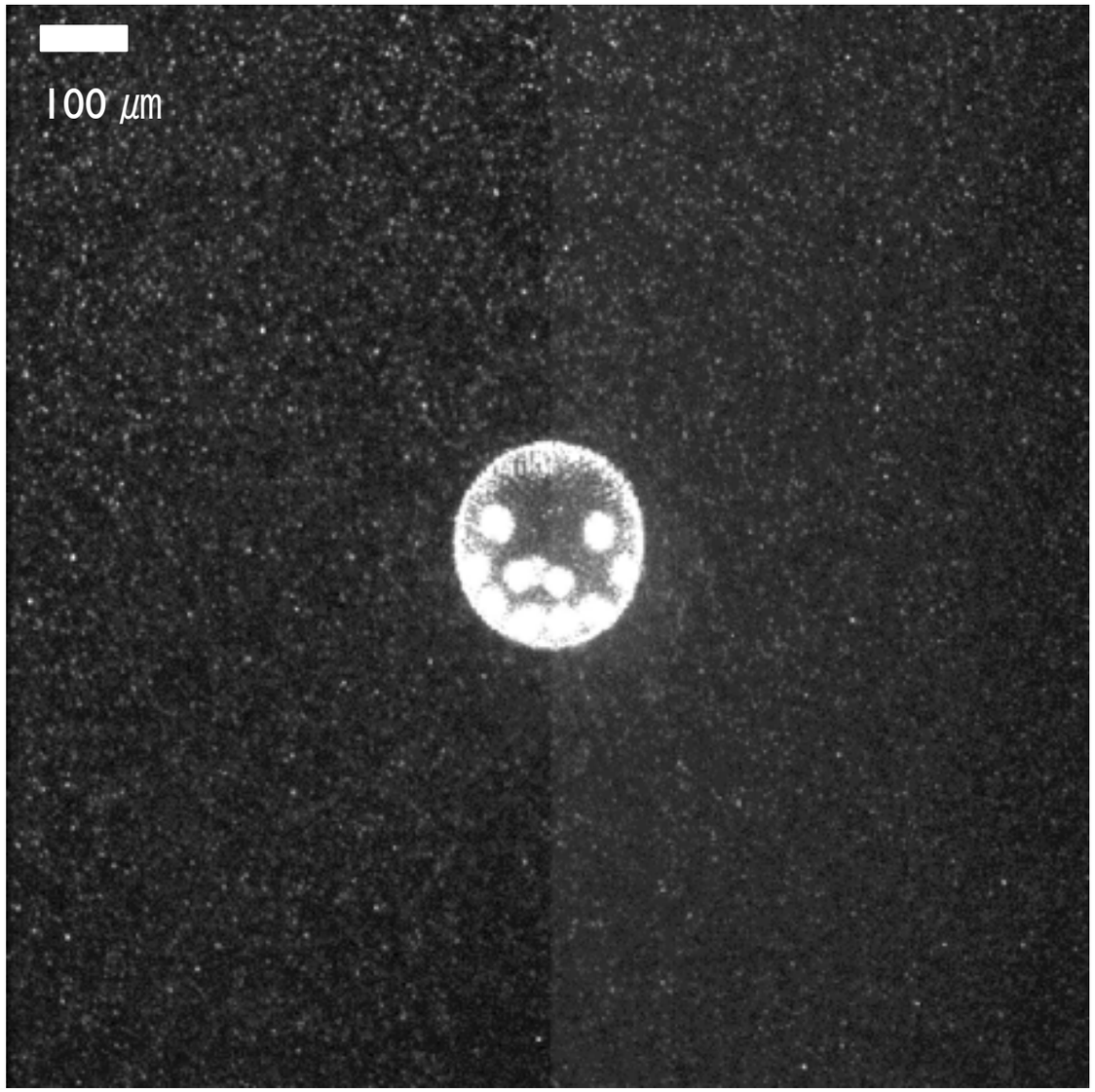
rotlet

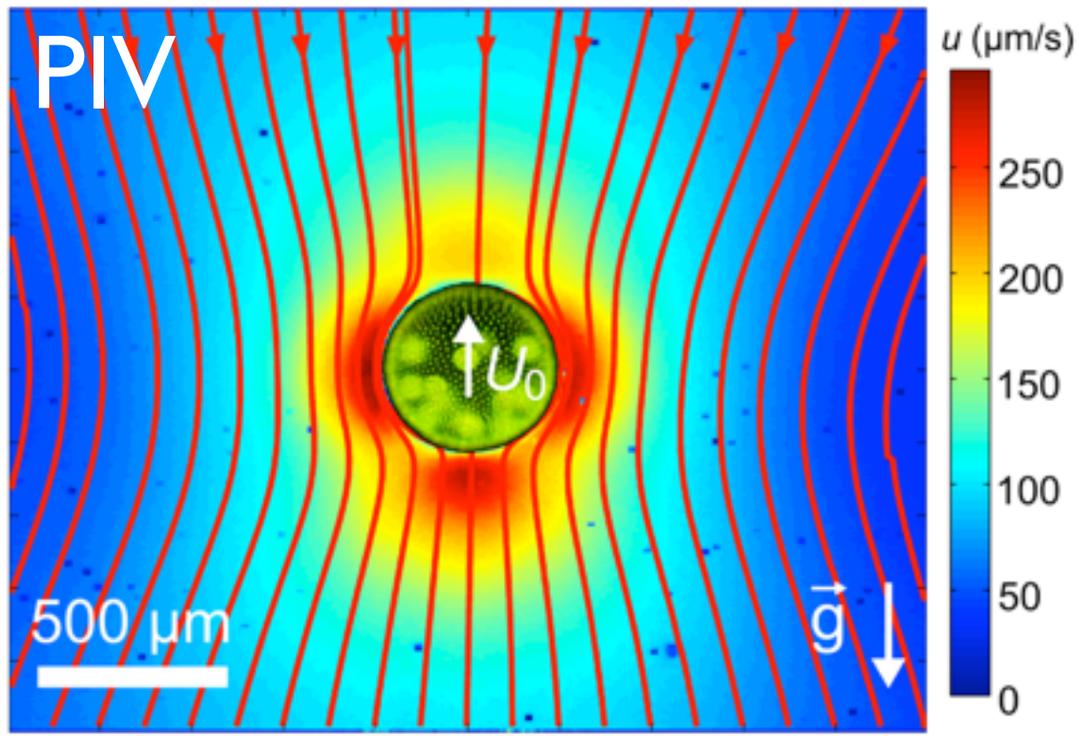


r^{-2}

Volvox carteri

swimming speed ~ 100 μm/sec





$$\mathbf{v}_{fit}(\mathbf{r}) = -\ U_0\,\hat{\mathbf{y}} - \frac{A_{St}}{r}\left(\mathbf{I}+\hat{\mathbf{r}}\hat{\mathbf{r}}\right)\cdot\hat{\mathbf{y}} \qquad (1)$$
$$+\ \frac{A_{str}}{r^2}\left(1-3(y/r)^2\right)\hat{\mathbf{r}} - \frac{A_{sd}}{r^3}\left(\frac{\mathbf{I}}{3}-\hat{\mathbf{r}}\hat{\mathbf{r}}\right)\cdot\hat{\mathbf{y}}$$

Drescher et al (2010) PRL

dunkel@math.mit.edu

How does *Volvox* achieve phototaxis ?

Approach:

- light response of individual cells
- effects of size & spinning frequency
- mathematical modeling
- check predictions of model

dunkel@math.mit.edu

Experimental setup

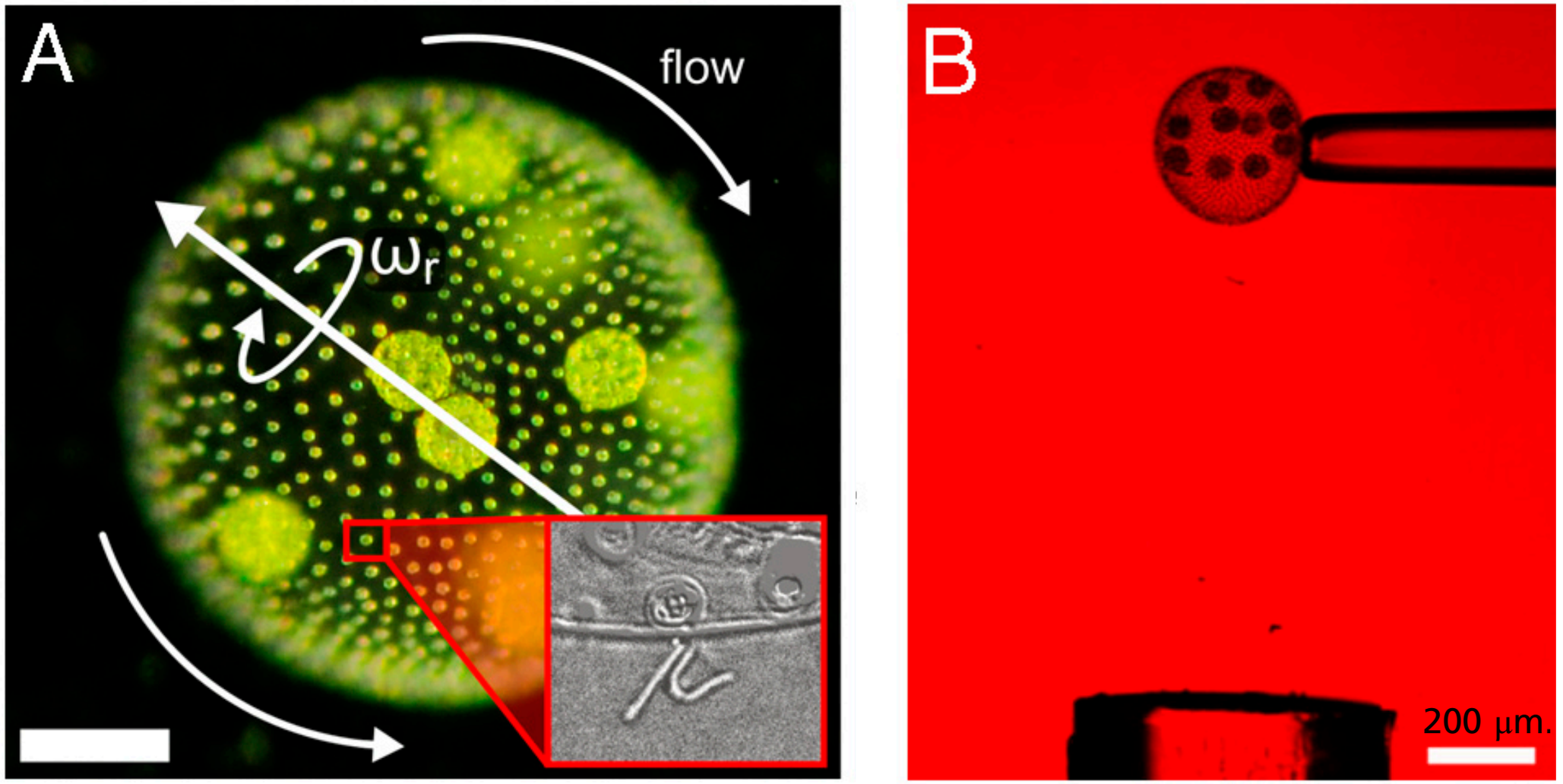
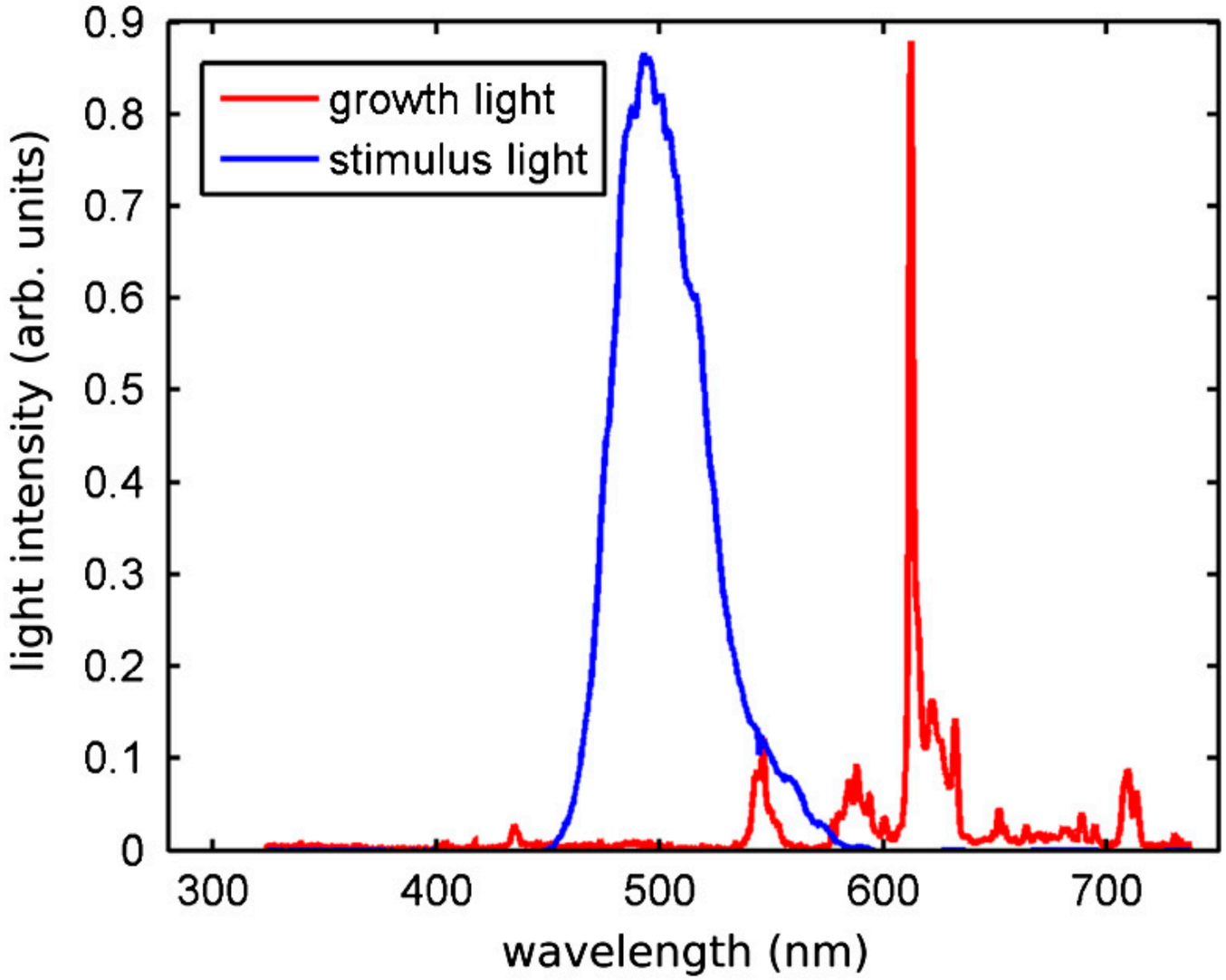


Fig. 1. Geometry of *V. carteri* and experimental setup. (*A*) The beating flagella, two per somatic cell (*Inset*), create a fluid flow from the anterior to the posterior, with a slight azimuthal component that rotates *Volvox* about its posterior-anterior axis at angular frequency ω_r. (Scale bar: 100 μm.) (*B*) Studies of the flagellar photoresponse utilize light sent down an optical fiber.

dunkel@math.mit.edu

Spectra of light sources



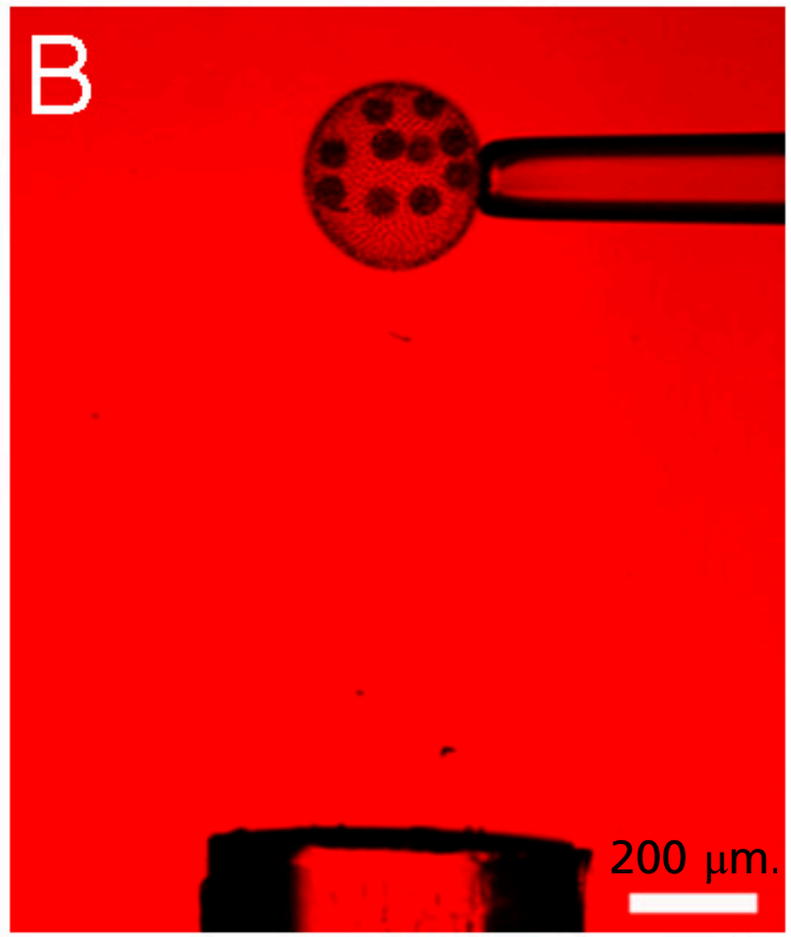
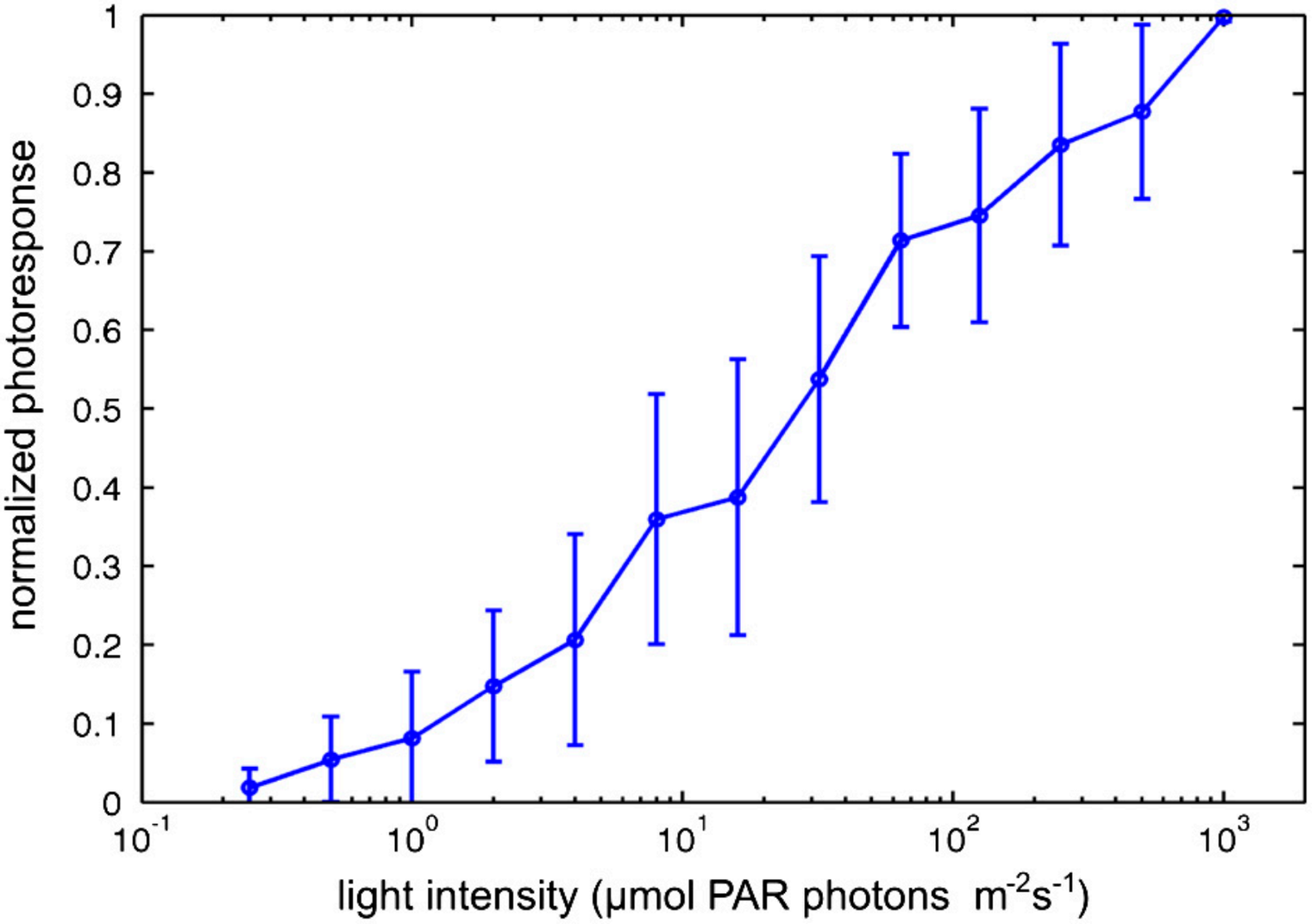


photo response via flow, 100 fps

dunkel@math.mit.edu

Photo-response at different intensities



0.25Hz

dunkel@math.mit.edu

Adaptive photo-response

$u_0 = 81$ μm/s

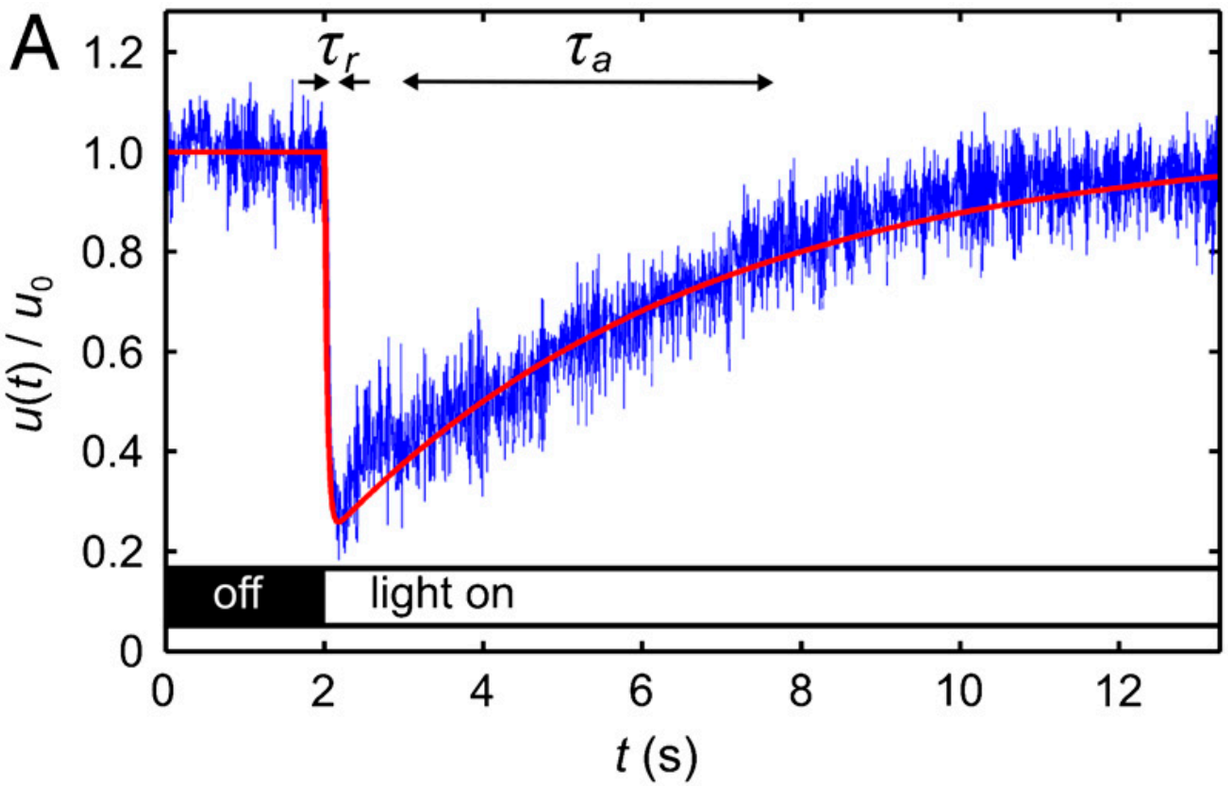
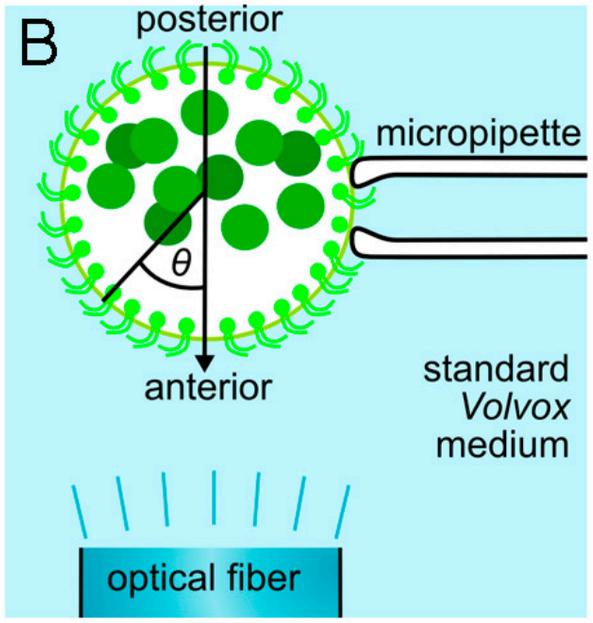


Fig. 2. Characteristics of the adaptive photoresponse. (*A*) The local flagella-generated fluid speed $u(t)$ (*Blue*), measured with PIV just above the flagella during a step up in light intensity, serves as a measure of flagellar activity. The baseline flow speed in the dark is $u_0 = 81$ μm/s for this dataset. Two time scales are evident: a short response time τ_r and a longer adaptation time τ_a. The fitted theoretical curve (*Red*) is from Eq. **4**. (*B*) The times τ_r (*Squares*) and τ_a (*Circles*) vary smoothly with the stimulus light intensity, measured in terms of PAR. Error bars are standard deviations.



1 μm tracers

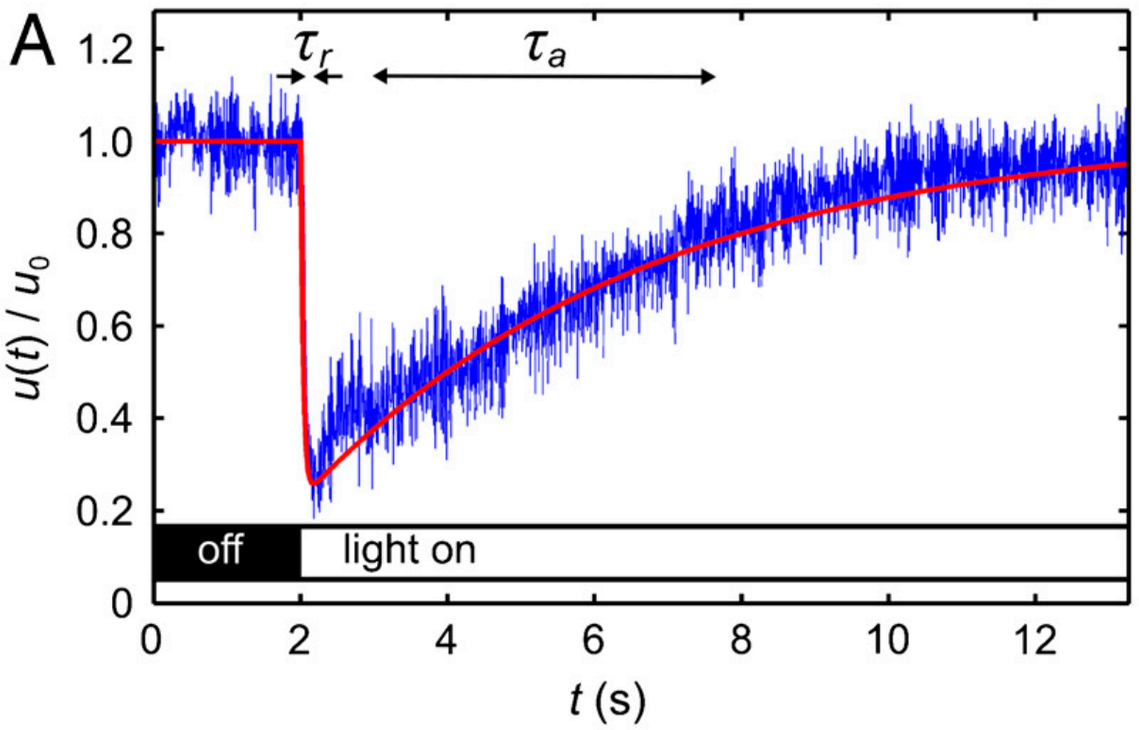
10μm from cilium

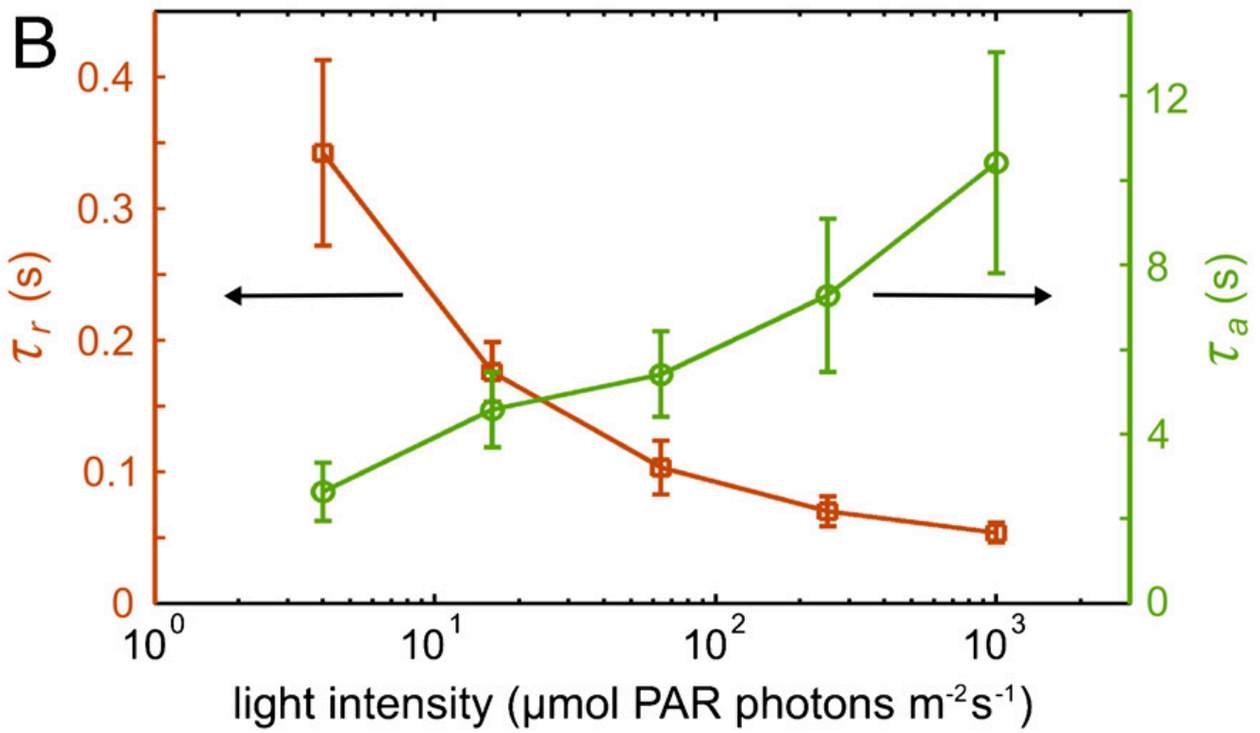
u(t) = average -30° ... +30°

dunkel@math.mit.edu

Adaptive photo-response

$u_0 = 81\ \mu\text{m/s}$





τ_r : Ca^{2+}-diffusion (?) ($L \sim 15\ \mu\text{m},\ D \sim 10^{-5}\ \text{cm}^2/\text{s}$)

τ_a : unknown

dunkel@math.mit.edu

Photo-response model

$u_0 = 81\ \mu\text{m/s}$

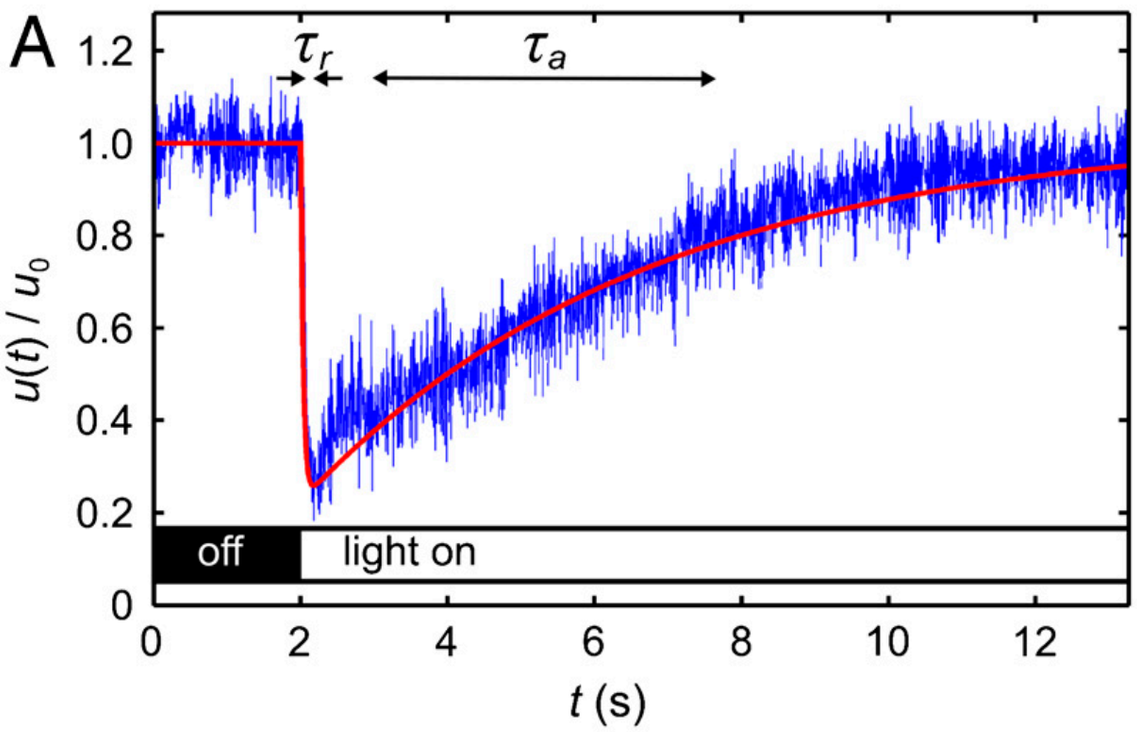


photo-response variable

$$u(t)/u_0 = 1 - \beta p(t)$$

$$\tau_r \dot{p} = (s-h)H(s-h) - p,$$

$$\tau_a \dot{h} = s - h,$$

$$h(t) = s_1 e^{-t/\tau_a} + s_2(1 - e^{-t/\tau_a}),$$

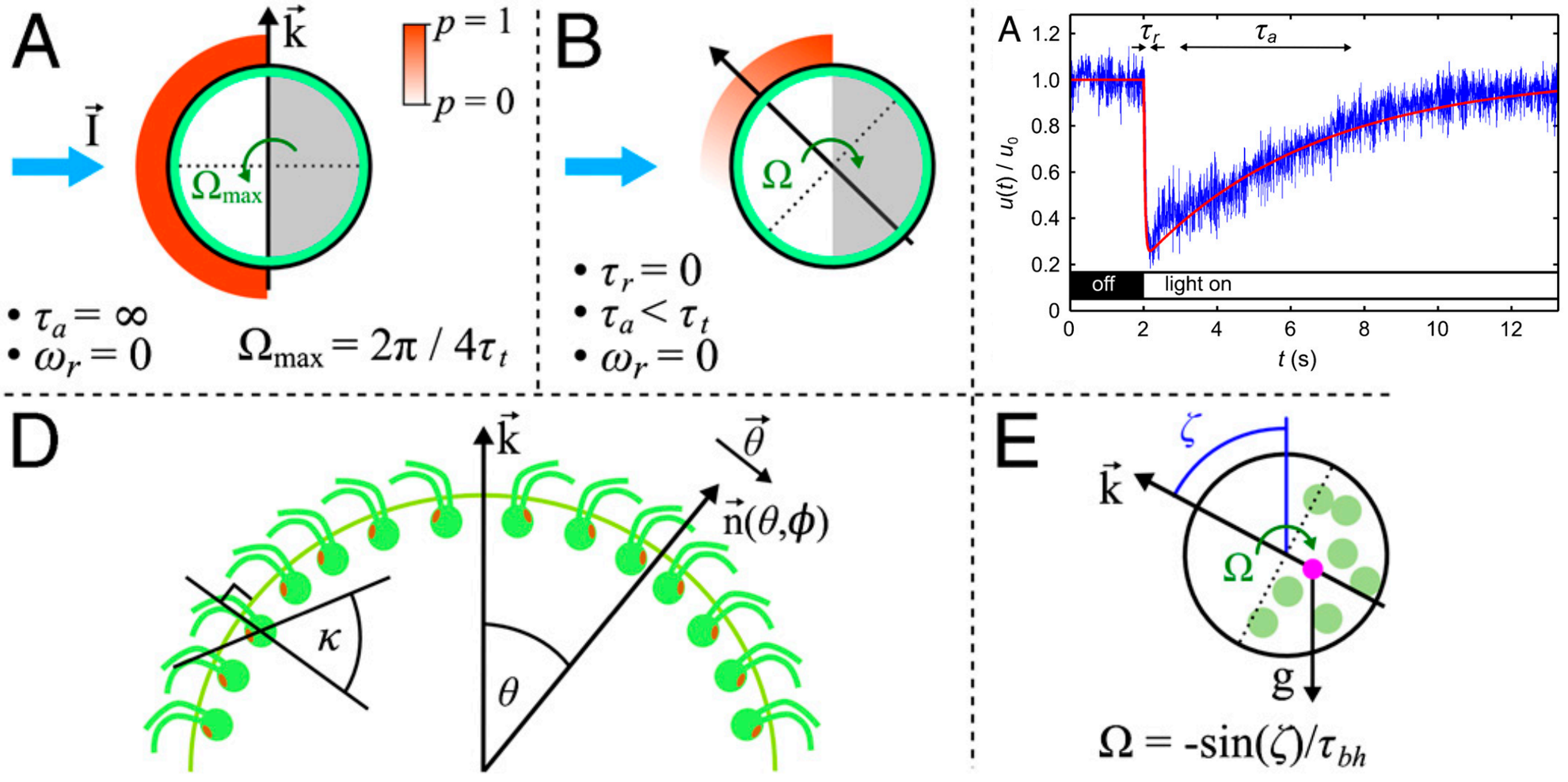
$$p(t) = \frac{(s_2 - s_1)}{1 - \tau_r/\tau_a}(e^{-t/\tau_a} - e^{-t/\tau_r}).$$

s: stimulus input variable

h: hidden biochemistry variable

dunkel@math.mit.edu

Heuristic response model



dunkel@math.mit.edu

Let's try to be more quantitative ...

dunkel@math.mit.edu

Frequency dependence of photo-response

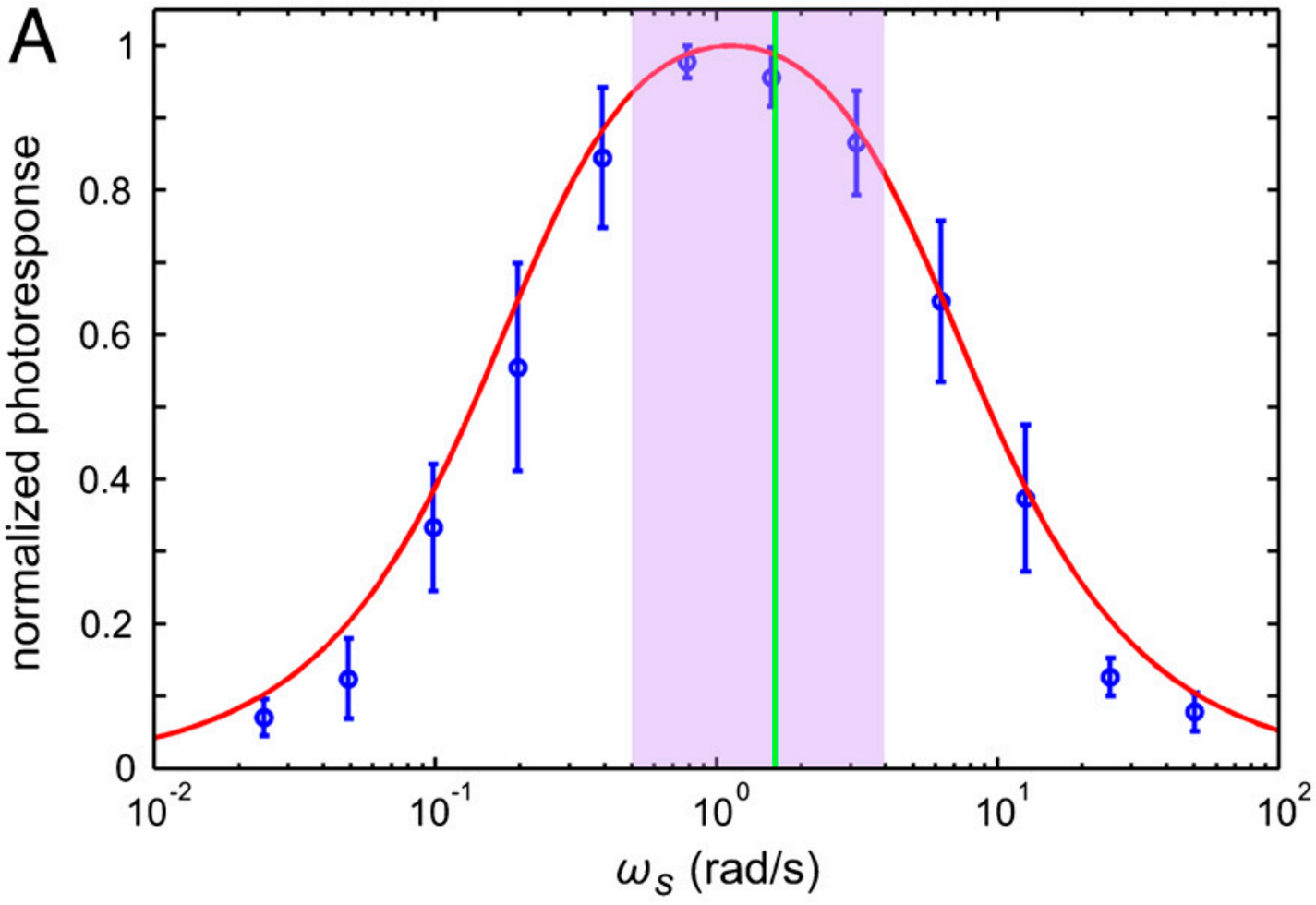


Fig. 3. Photoresponse frequency dependence and colony rotation. (*A*) The normalized flagellar photoresponse for different frequencies of sinusoidal stimulation, with minimal and maximal light intensities of 1 and 20 μmol PAR photons m^{-2} s^{-1} (*Blue Circles*). The theoretical response function (Eq. **5**, *Red Line*) shows quantitative agreement, using τ_r and τ_a from Fig. 2*B* for 16 μmol PAR photons m^{-2} s^{-1}.

dunkel@math.mit.edu

Frequency dependence of photo-response

FT depends on input signal

$$\mathscr{R} = |\tilde{p}/\tilde{s}|,$$

$$\tau_r \dot{p} = (s-h)H(s-h) - p,$$
$$\tau_a \dot{h} = s - h,$$

$$\mathscr{R}(\omega_s) = \frac{\omega_s \tau_a}{\sqrt{(1+\omega_s^2\tau_r^2)(1+\omega_s^2\tau_a^2)}}.$$

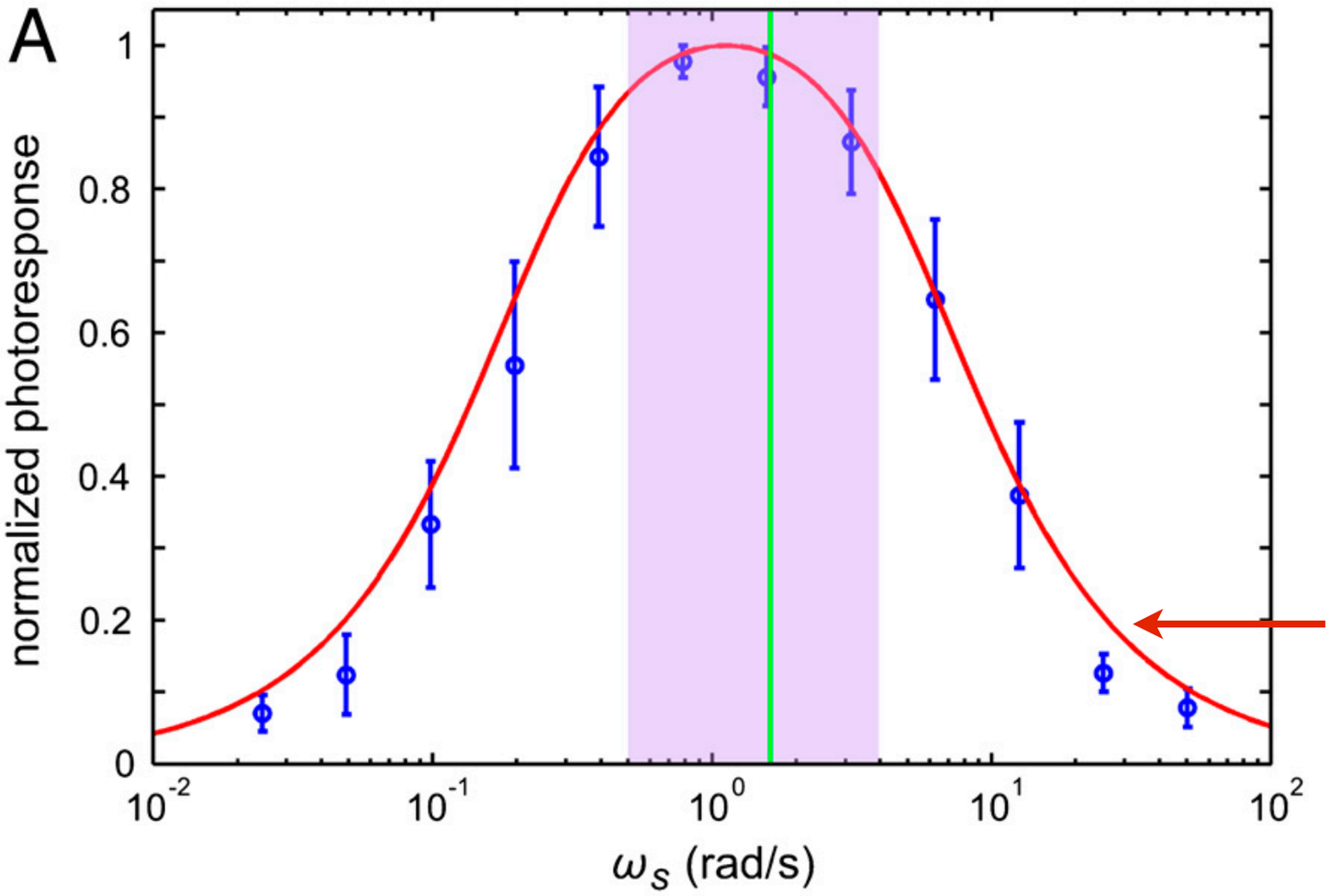
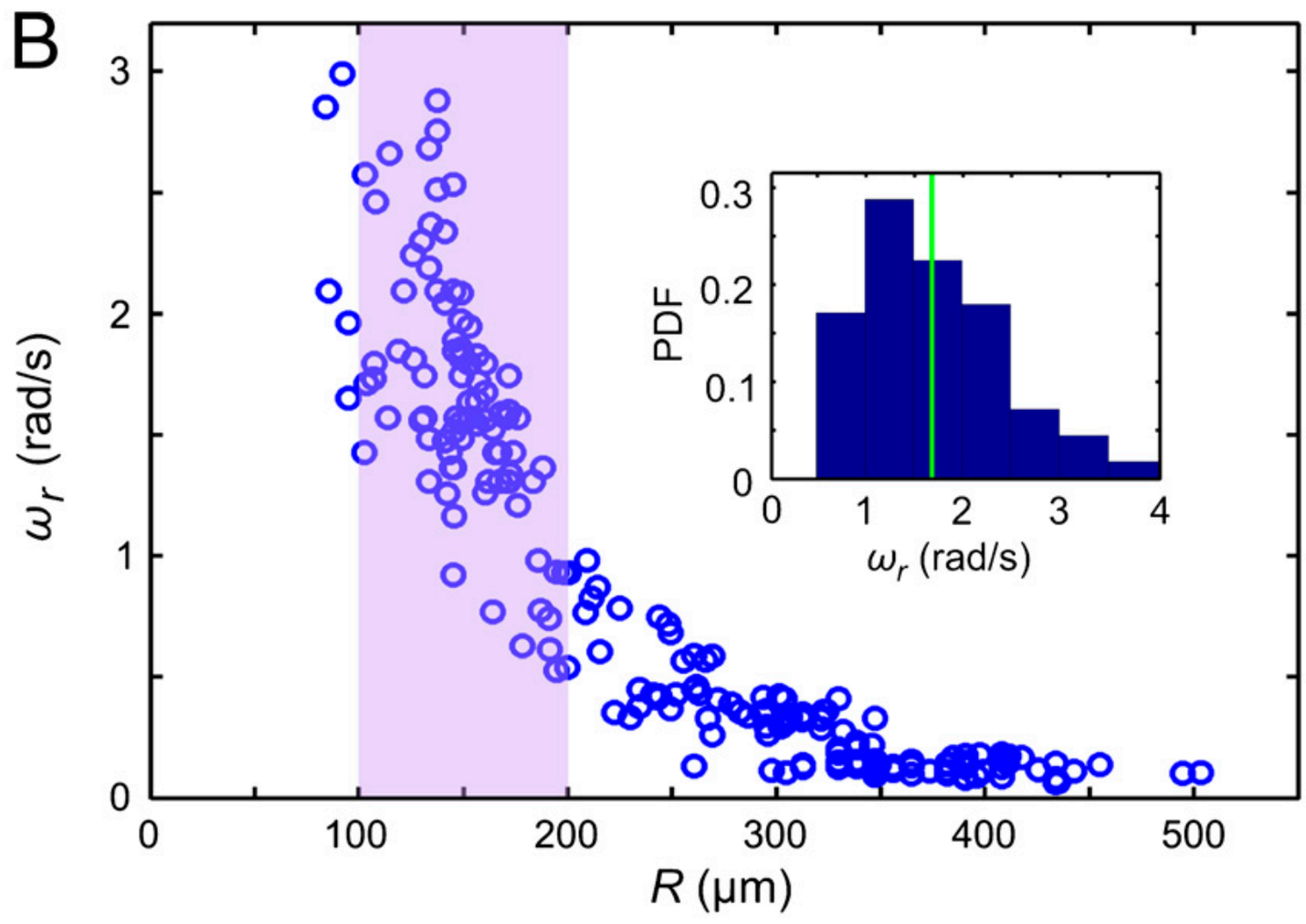


Fig. 3. Photoresponse frequency dependence and colony rotation. (*A*) The normalized flagellar photoresponse for different frequencies of sinusoidal stimulation, with minimal and maximal light intensities of 1 and 20 μmol PAR photons m^{-2} s^{-1} (*Blue Circles*). The theoretical response function (Eq. **5**, *Red Line*) shows quantitative agreement, using τ_r and τ_a from Fig. 2*B* for 16 μmol PAR photons m^{-2} s^{-1}.

dunkel@math.mit.edu

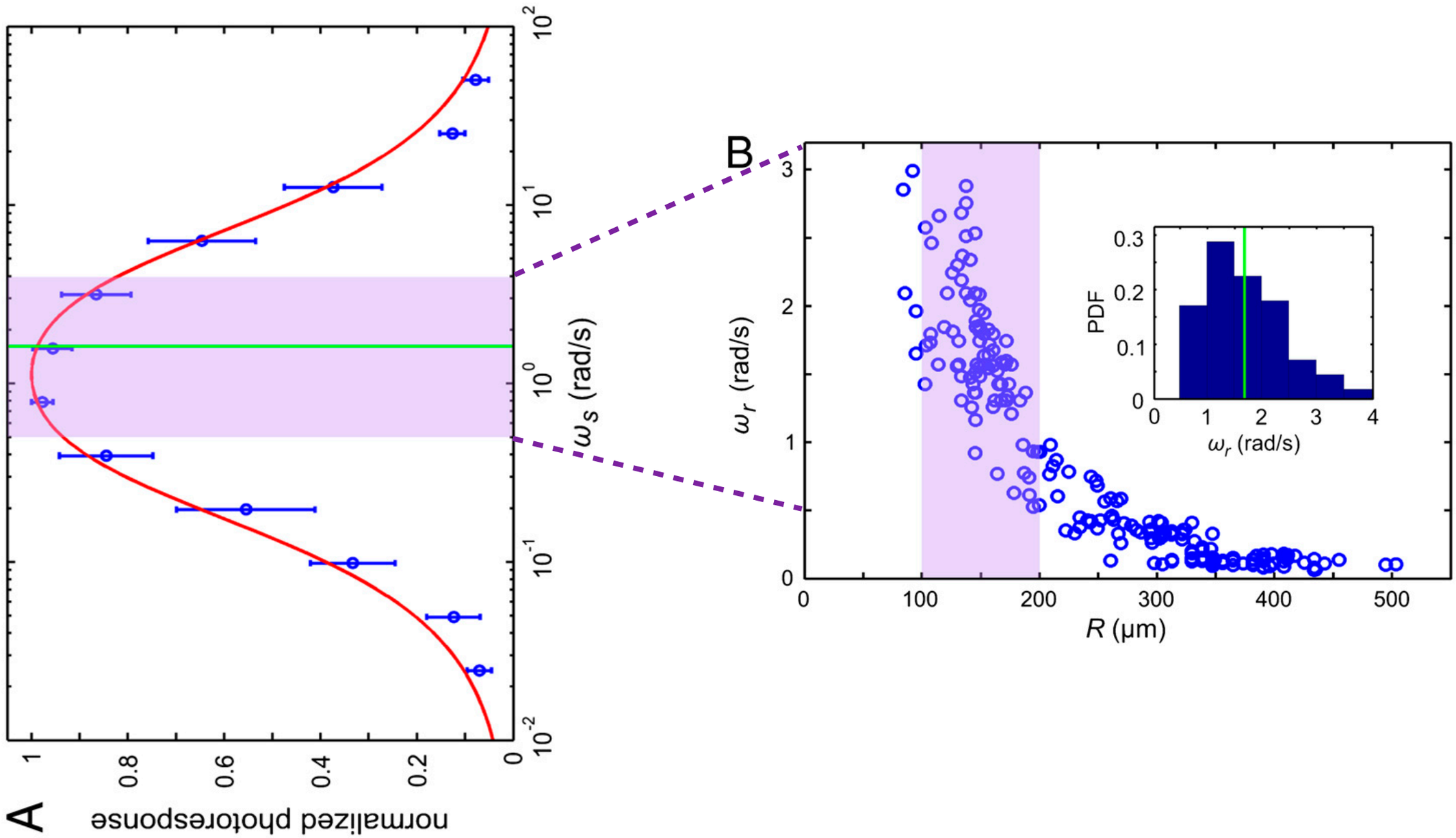
Spinning frequency *vs* size



(*B*) The rotation frequency ω_r of *V. carteri* as a function of colony radius *R*. The highly phototactic organisms for which photoresponses were measured fall within the range of *R* indicated by the purple box, and the distribution of *R* can be transformed into an approximate probability distribution function (PDF) of ω_r (*Inset*), by using the noisy curve of $\omega_r(R)$. The purple box in *A* marks the range of ω_r in this PDF (green line indicates the mean), showing that the response time scales and colony rotation frequency are mutually optimized to maximize the photoresponse.

dunkel@math.mit.edu

Optimal response !



dunkel@math.mit.edu

How about spatial structure ?

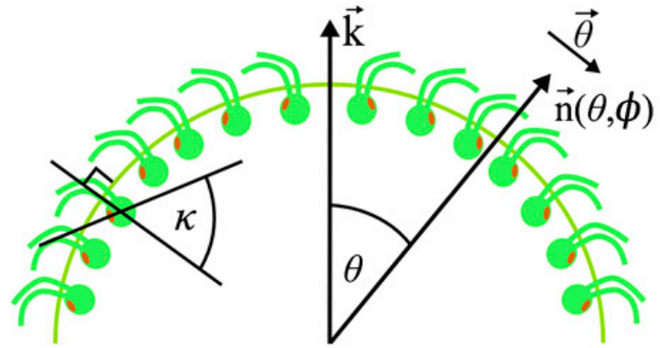
dunkel@math.mit.edu

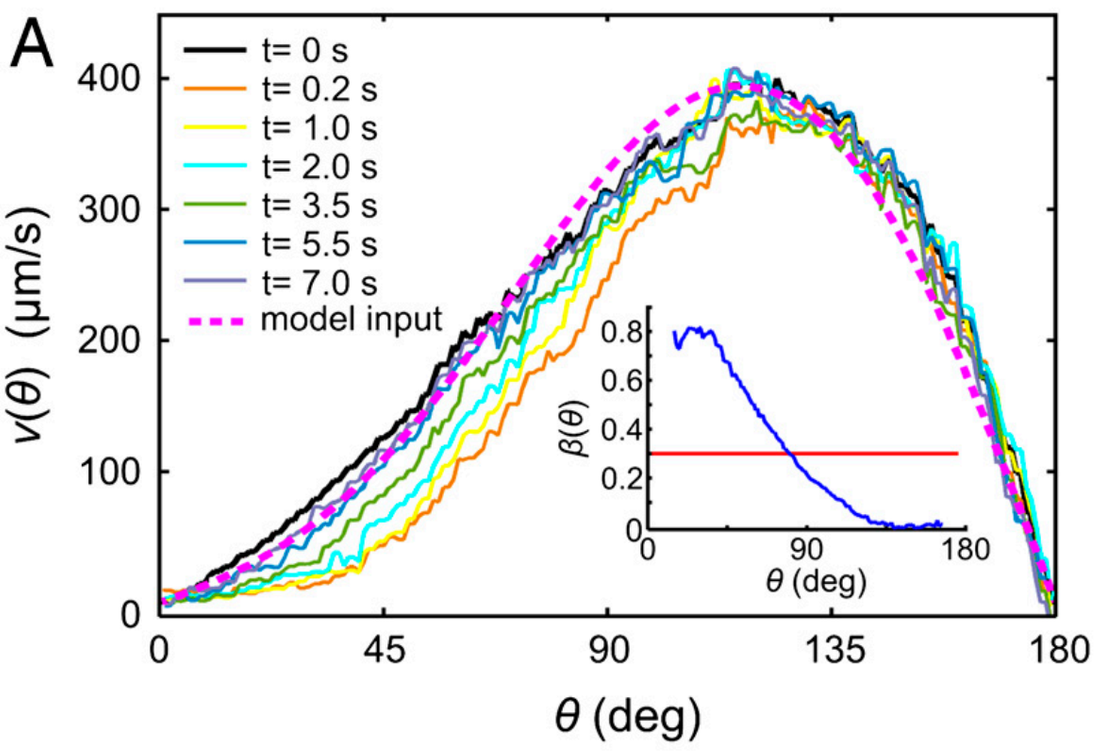
Front-back asymmetry

$$\mathbf{u} = v\hat{\boldsymbol{\theta}} + w\hat{\boldsymbol{\phi}}.$$

$$u(t)/u_0 = 1 - \beta p(t)$$

ratio $v_0(\theta)/w_0(\theta)$ is constant on the colony surface





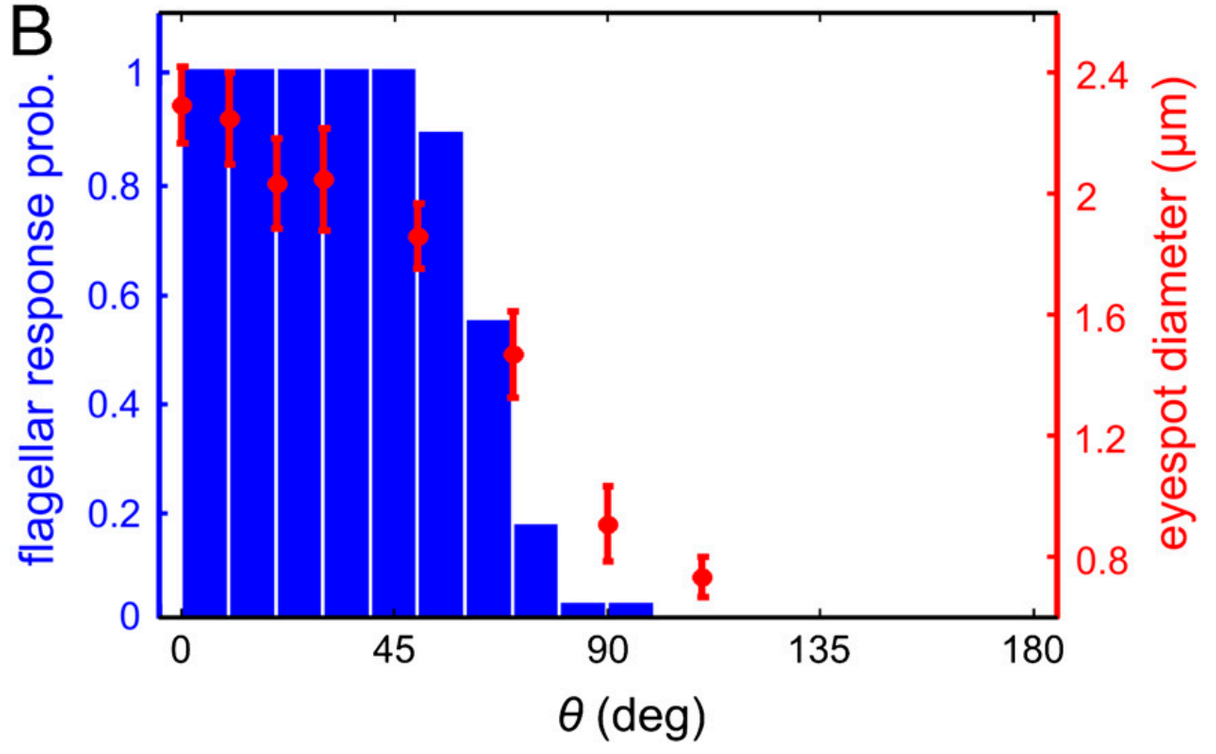


Fig. 5. Anterior-posterior asymmetry. (*A*) The anterior-posterior component of the fluid flow, measured 10 μm above the beating flagella, following a step up in illumination at time $t = 0$ s. The dashed line indicates the approximation to $v_0(\theta)$ used in the numerical model. (*Inset*) $\beta(\theta)$ is blue (with p normalized to unity), and the mean β is red. (*B*) The probability of flagella to respond to light correlates with the size of the somatic cell eyespots. The light-induced decrease in fluid flow occurs beyond the region of flagellar response because of the nonlocality of fluid dynamics.

dunkel@math.mit.edu

Eye-spot measurements

anterior pole

θ=0 θ=50° $\kappa = 57° \pm 7°$

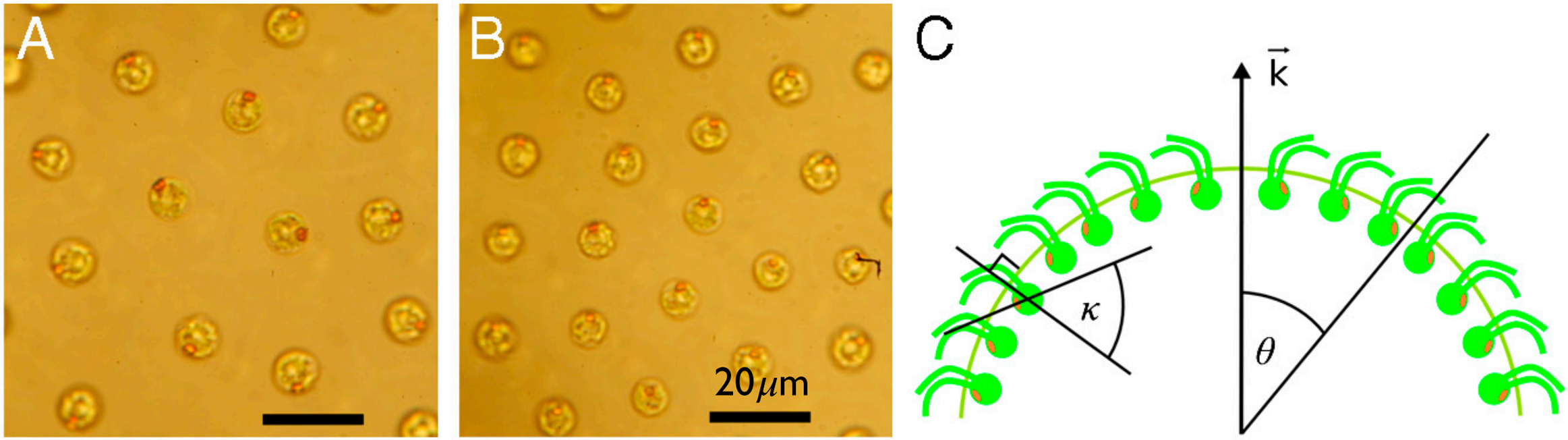


Fig. S5. (*A*) The *V. carteri* somatic cells at the anterior pole have their orange eyespots facing away from the fluid-mechanical anterior pole. (*B*) The somatic cells and eyespots at polar angle $\theta = 50°$ from the anterior. (Scale bars: 20 μm.) (*C*) Illustration of the eyespot placement in the somatic cells and the relation to the posterior-anterior axis **k**. In contrast to this schematic drawing, *V. carteri* colonies consist of thousands of somatic cells, as shown in Fig. 1*A* of the main text and as measured in ref. 20.

dunkel@math.mit.edu

Basic ingredients of a‘full’ model

- self-propulsion
- bottom-heaviness
- photo-response kinetics
- photo-response spatial variation

dunkel@math.mit.edu

Hydrodynamic model

$$\tau_r \dot{p} = (s-h)H(s-h) - p,$$
$$\tau_a \dot{h} = s - h,$$

$$s(\theta,\phi,\hat{\mathbf{l}}) = f(\psi)H(\cos\psi)$$

$$\psi(\theta,\phi,\hat{\mathbf{l}})$$
$$\cos\psi = -\hat{\mathbf{n}}\cdot\hat{\mathbf{l}},$$

$$\mathbf{u}(\theta,\phi,t) = \mathbf{u}_0(\theta)[1-\beta(\theta)p(\theta,\phi,t)],$$

$$f(\psi) = \cos\psi$$
$$\beta(\theta)$$

$$\mathbf{U}(t) = \frac{1}{4\pi R^2}\int \mathbf{u}(\theta,\phi,t)dS,$$

$$\mathbf{\Omega}(t) = \frac{1}{\tau_{\text{bh}}}\hat{\mathbf{g}}\times\hat{\mathbf{k}} - \frac{3}{8\pi R^3}\int \hat{\mathbf{n}}\times\mathbf{u}(\theta,\phi,t)dS$$

VS

$$f(\psi) = 1$$
$$\beta(\theta) = 0.3$$

Stone HA, Samuel ADT (1996) Propulsion of microorganisms by surface distortions. *Phys Rev Lett* 77:4102–4104.

dunkel@math.mit.edu

‘Simple’ squirmer model

no eye-spot directionality

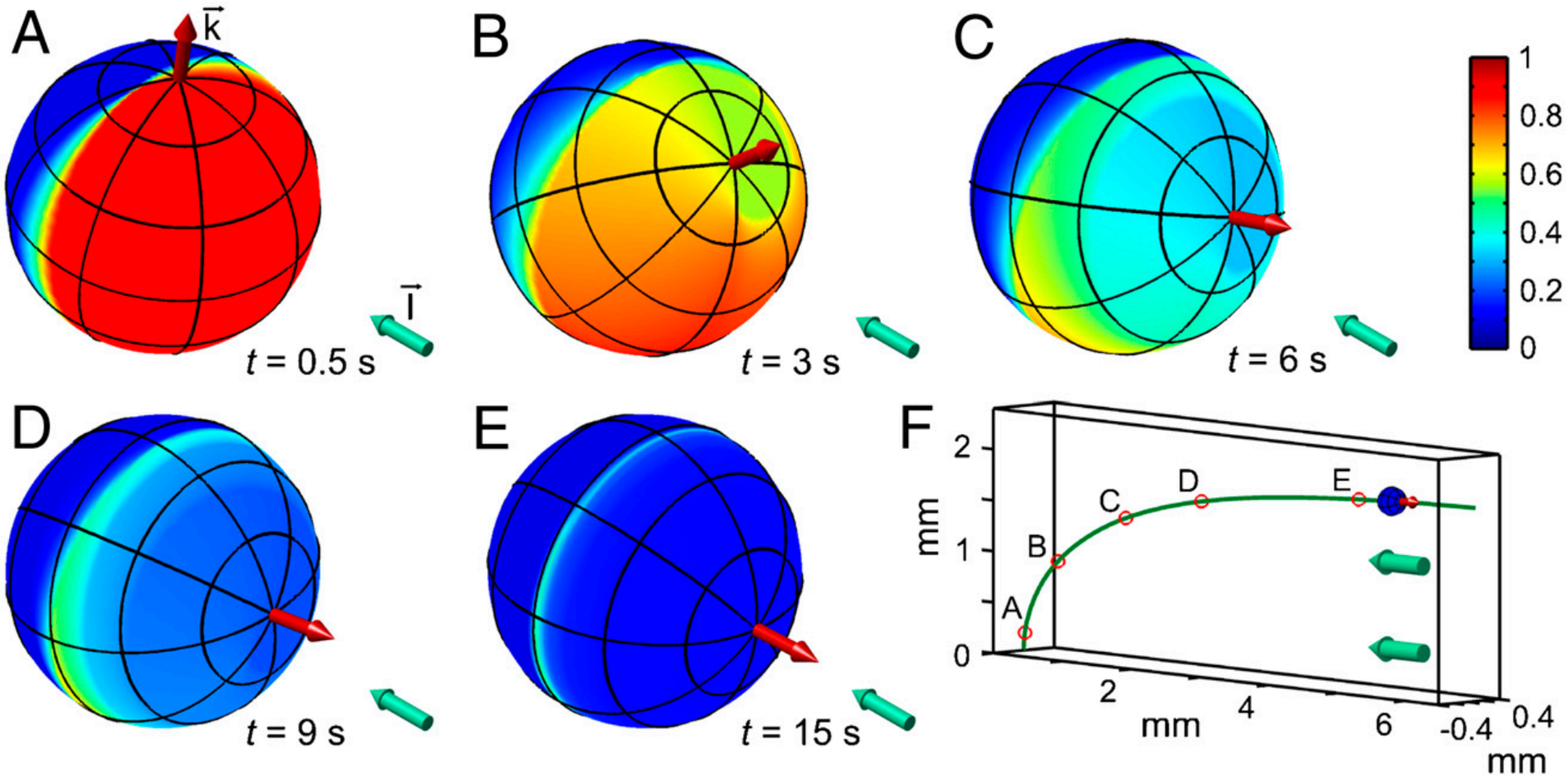


Fig. 6. Colony behavior during a phototurn. *A–E* show the colony axis **k** (*Red Arrow*) tipping toward the light direction **l** (*Aqua Arrow*). Colors represent the amplitude $p(t)$ of the down-regulation of flagellar beating in a simplified model of phototactic steering. *F* shows the location of colonies in *A–E* along the swimming trajectory.

dunkel@math.mit.edu

‘Full’ squirmer model

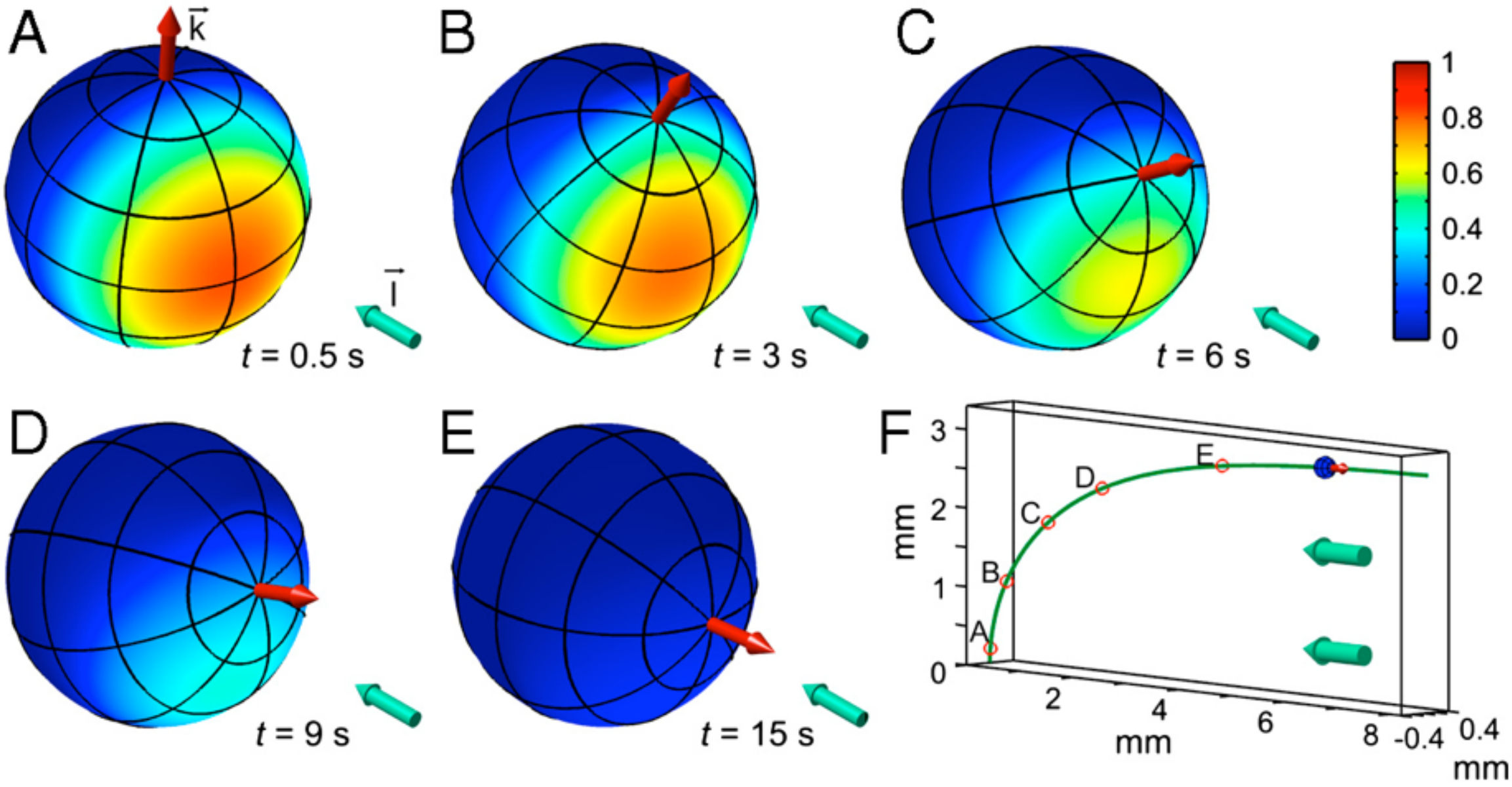
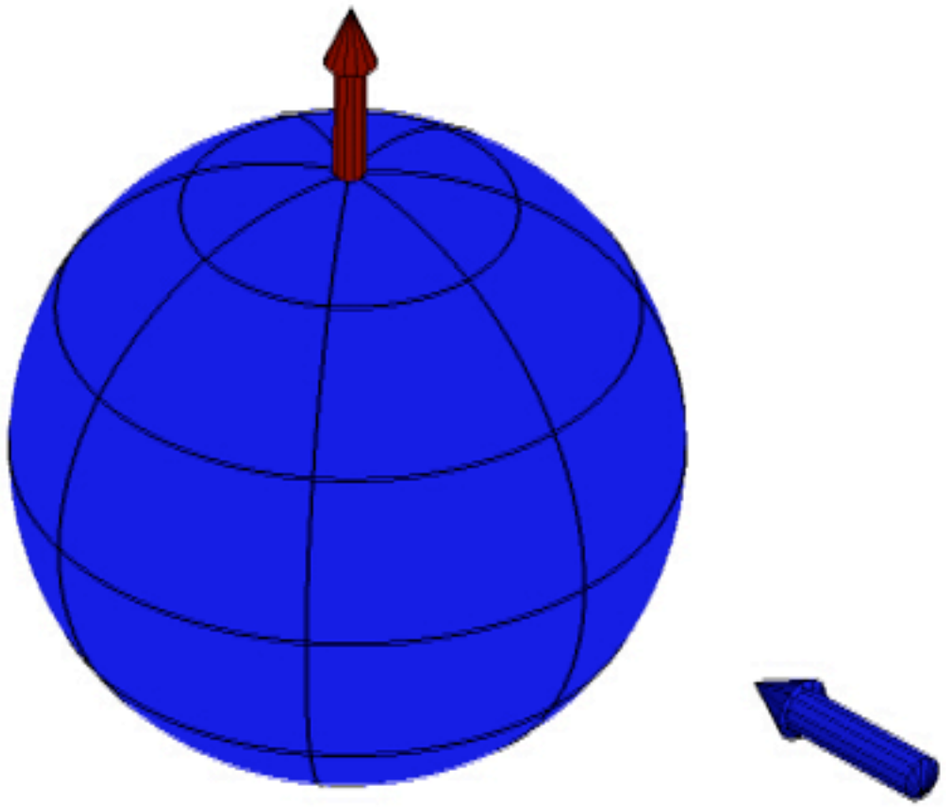


Fig. S8. The behavior of the photoresponse $p(\theta,\phi,t)$ during a phototactic turn, using the full model defined in the main text, neglecting bottom-heaviness. *A–E* show the colony axis (*Red Arrow*) tipping toward the direction of light (*Aqua Arrow*) over time. The color scheme illustrates the magnitude of *p*. *F* shows the location of colonies in *A–E* along the swimming trajectory.

dunkel@math.mit.edu

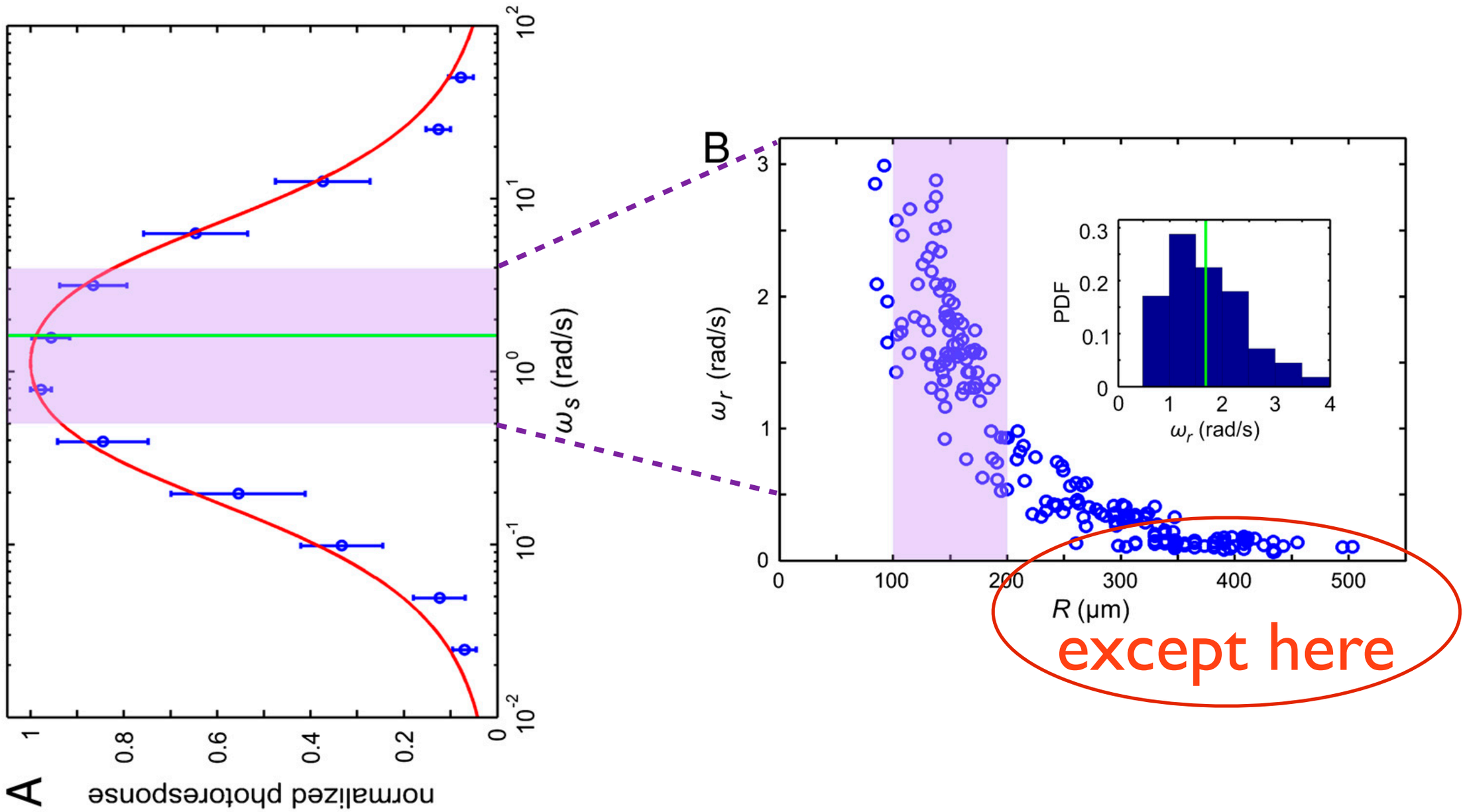
Squirmer model



movie provided by K. Drescher

dunkel@math.mit.edu

Optimal response !



dunkel@math.mit.edu

Phototactic ability decreases with rotation frequency

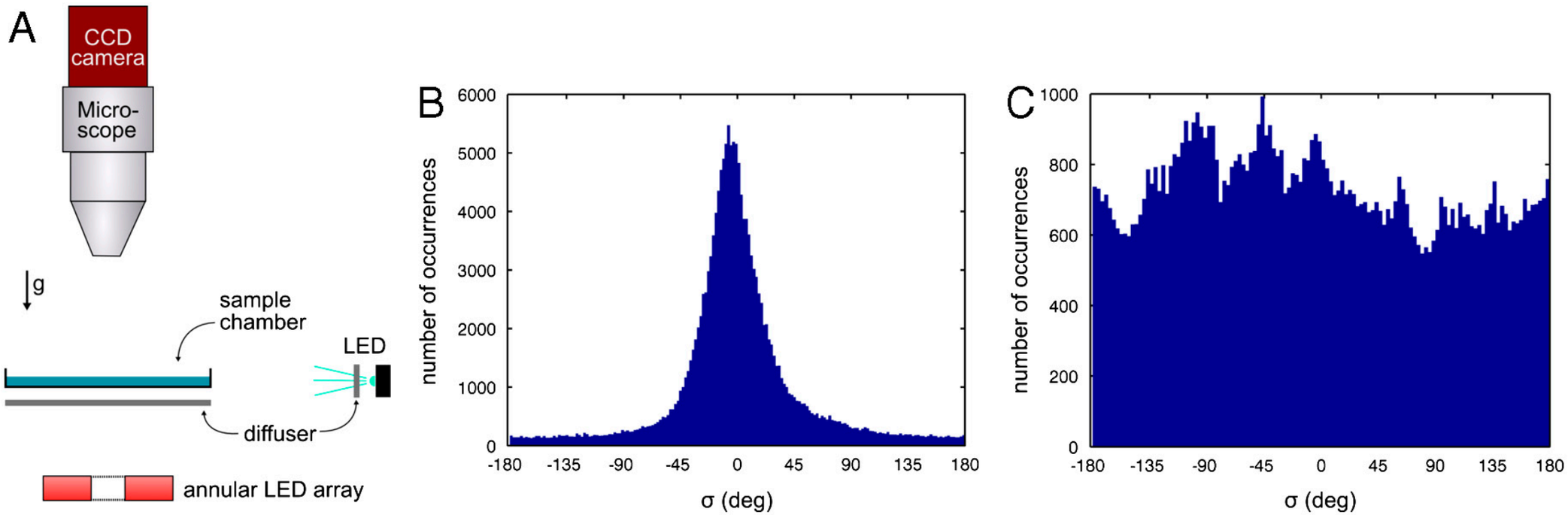


Fig. S6. (*A*) Schematic diagram of the apparatus used for the population assay. *B* and *C* show distributions of the swimming angle with the light direction σ as measured for a population at the viscosity of water (*B*) and at 40 times the viscosity of water (*C*).

dunkel@math.mit.edu

Phototactic ability decreases with rotation frequency

$$\mathscr{A} = (\text{swimming speed toward the light})/(\text{swimming speed})$$

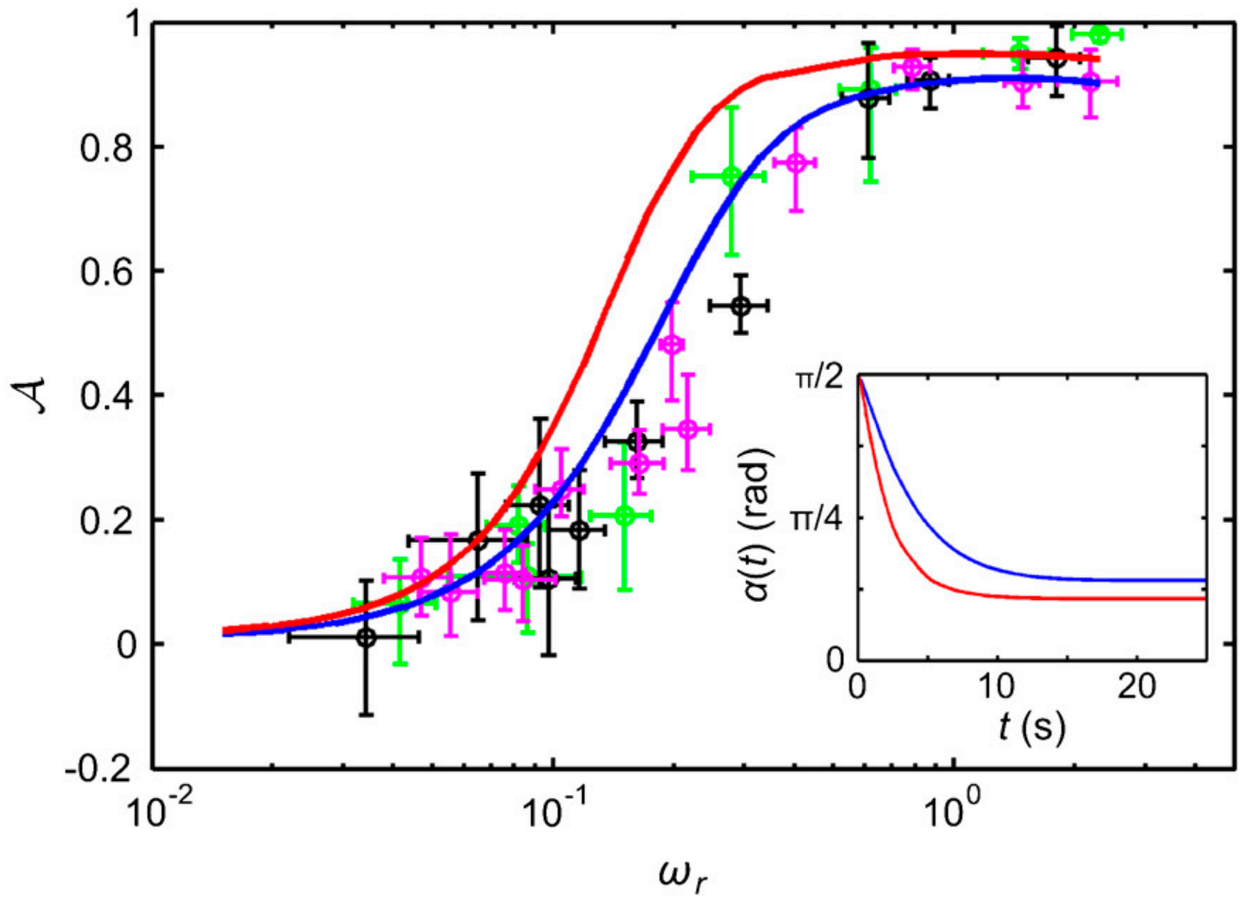


Fig. 7. The phototactic ability $\mathscr{A}$ decreases dramatically as ω_r is reduced by increasing the viscosity. Results from three representative populations are shown with distinct colors. Each data point represents the average phototactic ability of the population at a given viscosity. Horizontal error bars are standard deviations, whereas vertical error bars indicate the range of population mean values, when it is computed from 100 random selections of 0.1% of the data. A blue continuous line indicates the prediction of the full hydrodynamic model; the red line is obtained from the reduced model. (*Inset*) $\alpha(t)$ from the full and reduced model at the lowest viscosity.

tuning ω_r via viscosity increase

dunkel@math.mit.edu

Open questions

- not all somatic cells photo-responsive ... why ?
- what determines τ_a ?
- chemotaxis *vs* phototaxis
- effects of (intrinsic) noise
- *Chlamydomonas* behave similarly ... generic *?*
- artificial steering devices

dunkel@math.mit.edu